Ministry for Primary Industries
Manatū Ahu Matua

The 2015 stock assessment of paua (*Haliotis iris*) for PAU 7

New Zealand Fisheries Assessment Report 2016/35

D. Fu

ISSN 1179-5352 (online)
ISBN 978-1-77665-287-7 (online)

June 2016

New Zealand Government

Growing and Protecting New Zealand

Requests for further copies should be directed to:

Publications Logistics Officer
Ministry for Primary Industries
PO Box 2526
WELLINGTON 6140

Email: brand@mpi.govt.nz
Telephone: 0800 00 83 33
Facsimile: 04-894 0300

This publication is also available on the Ministry for Primary Industries websites at:
http://www.mpi.govt.nz/news-resources/publications.aspx
http://fs.fish.govt.nz go to Document library/Research reports

Contents

EXECUTIVE SUMMARY

Fu, D. (2016). The 2015 stock assessment of paua (*Haliotis iris*) for PAU 7.

***New Zealand Fisheries Assessment Report 2016/35*. 52 p.**

This report summarises the stock assessment for PAU 7 which includes fishery data up to the 2014–15 fishing year. The report describes the model structure and output, including current and projected stock status. The stock assessment is implemented as a length-based Bayesian estimation model, with point estimates of parameters based on the mode of the joint posterior distribution, and uncertainty of model estimates investigated using the marginal posterior distributions generated from Markov chain-Monte Carlo simulation.

The data fitted in the assessment model were: (1) a standardised CPUE series based on the early CELR data, (2) a standardised CPUE series based on recent PCELR data, (3) commercial catch sampling length frequency series (CSLF), (4) tag-recapture length increment data, (5) maturity-at-length data (6) length frequency data from the Fighting Bay fish-down experiment. The Fighting Bay length frequency was assumed to represent the length distribution from an equilibrium unfished population. The research diver survey data were not used in this assessment because there is concern that the data are not a reliable index of abundance. Results from the previous assessment suggested the inclusion of the research diver survey indices had little influence on estimates of stock status.

The base case model (1.0) estimated that the spawning stock population in 2015 (B_{2015}) was 18% (16–21%) of B_0. The model projection made for three years using recruitment re-sampled from a period with both high and low recruitment (2002–2011), suggested that the spawning stock abundance will increase to 22% (16–29%) of B_0 in 2018 if the future catch remains at the current level (corresponding to a 28% TACC reduction), or 24% (18–31%) of B_0 if the future catch is reduced to 50% of the TACC. The projections using recruitment re-sampled from the recent period with low recruitment (2010–2011), suggested that the spawning stock abundance will only increase to 19% (14–25%) of B_0 in 2018 if the future catch remains at the current level, or 21% (16–27%) of B_0 with a 50% TACC reduction. It was extremely unlikely that the stock status will be above the target (40% B_0) in the short term.

The assessment indicates that the stock abundance has declined since 2010 and the current stock status is probably below the soft limit (20% B_0). The decline of abundance in recent years has been corroborated by the observed trend in both CPUE and length frequencies from the commercial fishery. The estimate of stock status is reasonably robust to various model assumptions made in the assessment, and the MPD estimate of B_{2015} ranges from 17% to 21% B_0 across sensitivity trials.

Most data used in the model were collected across the stock areas and are believed to be representative of the population. However, there is also a great deal of uncertainty on some key demographic parameters such as natural mortality and growth. The assessment has considered a procedure to develop a prior distribution on natural mortality using posterior estimates from assessments of other QMA stocks (i.e. PAU 5A and 5B), as recommended by the paua review expert panel. This procedure produced a prior with a higher mean and a larger CV than that assumed in the base case (model 1.0), leading to a slightly more optimistic estimate of stock status with wider bounds. The tag-recapture data have been weighted by the catch in each region when fitted in the model, and the estimates of growth were driven by data from the more productive southern area which contributed most of the catch in PAU 7. The estimated growth rates were consistent with the length

frequency derived from the Fighting Bay fish-down experiment, which is believed to represent the length distribution of an unfished population.

1. INTRODUCTION

1.1 Overview

This report summarises the stock assessment for PAU 7 (at the northern end of the South Island, Figure 1) with the inclusion of data to the end of the 2014–15 fishing year. The report describes the model structure and output, including current and projected stock status. The stock assessment is conducted with the length-based Bayesian estimation model first used in 1999 for PAU 5B (Breen et al. 2000a) with revisions made for subsequent assessments in PAU 5B (Breen et al. 2000b, Breen & Smith 2008a, Fu 2014a), PAU 4 (Breen & Kim 2004a), PAU 5A (Breen & Kim 2004b, Breen & Kim 2007, Fu & Mackenzie 2010a, b, Fu 2015a, 2015b), PAU 5D (Breen et al. 2000a, Breen & Kim 2007, Fu 2013), PAU 7 (Andrew et al. 2000, Breen et al. 2001, Breen & Kim 2003, 2005, McKenzie & Smith 2009a, Fu 2012), and PAU 3 (Fu 2014b). PAU 7 was last assessed in 2011 (Fu 2012, Fu et al. 2012). The model was published by Breen et al. (2003).

Most catches have been taken from Statistical Areas 017 and 038 (Figure 2). A different minimum harvest size is operating outside these two statistical areas (See Fu et al. 2016). Breen et al. (2001), Breen & Kim (2003, 2005), McKenzie & Smith (2009), and Fu (2012) based their assessments on Statistical Areas 017 and 038 only. The Shellfish Fishery Assessment Working Group agreed to continue this practice for this assessment.

The six sets of data used in the assessment were: (1) a standardised CPUE series covering 1990–2001 based on CELR data (CPUE), (2) a standardised CPUE series covering 2002–2015 based on PCELR data (PCPUE), (3) a commercial catch sampling length frequency series (CSLF), (4) tag-recapture length increment data, (5) maturity-at-length data, and (6) length frequency data from the Fighting Bay fish-down experiment. Catch history was an input to the model, encompassing commercial, recreational, customary, and illegal catch. Another document describes the datasets that are used in the stock assessment and the updates that were made from the previous assessment (Fu et al. 2016).

There have been concerns over the research diver survey methodology and its usefulness in providing relative abundance indices (Cordue 2009, Haist 2010). In the most recent stock assessments of PAU 5A, (Fu 2015a, b), PAU 5B (Fu 2014a) and PAU 5D (Fu 2013) the research diver survey indices (RDSI) and research diver survey length frequency (RDLF) data were not included in the base case. A sensitivity analysis from the previous PAU 7 assessment (Fu 2012) suggested that both the survey abundance indices and length frequencies have very little influence on estimated stock status due to the large variability associated with these data. There have been no new research diver surveys since 2005. Therefore the RDSI and RDLF were not used in this assessment. This assessment has included the Fighting Bay length frequency (FBLF, derived from a fish-down experiment, see Abraham (2012)), which is assumed to represent the length distribution from the unfished population (see Fu submitted for details).

The assessment was made in several steps. First, the model was fitted to the data with parameters estimated at the mode of their joint posterior distribution (MPD). Next, from the resulting fit, Markov chain-Monte Carlo (MCMC) simulations were made to obtain a large set of samples from the marginal posterior distribution. From this set of samples, forward projections were made with a set of agreed indicators obtained. Sensitivity trials were explored by comparing MPD fits made with alternative model assumptions. MCMC simulations were also taken for a number of sensitivity trials.

This document describes the model structure and assumptions, the fits to the data, estimates of parameters and indicators, and projection results. This report fulfils part of Objective 1 "Undertake a

stock assessment for PAU 7, using a length-based Bayesian model" of the Ministry for Primary Industries Project PAU201501.

1.2 Description of the fishery

The paua fishery was summarised by Schiel (1992), and in numerous previous assessment documents (e.g., Schiel 1989, McShane et al. 1994, 1996, Breen et al. 2000a, 2000b, 2001, Breen & Kim 2003, 2004a, 2004b, 2007, Breen & Smith 2008b, McKenzie & Smith 2009b, Fu et al. 2010, 2012, 2013, 2014a,b, 2015). A summary of the PAU 7 fishery up to the 2014–15 fishing year is presented in Fu et al. (2016).

2. MODEL

This section gives an overview of the model used for the stock assessment of PAU 5A in 2014; for full description see Breen et al. (2003). The model was developed for use in PAU 5B in 1999 and has been revised each year for subsequent assessments, in many cases echoing changes made to the rock lobster assessment model (Kim et al. 2004), which is a similar but more complex length-based Bayesian model. The last revision made to the model was in 2013 for the assessment of PAU 5B (Fu 2014a).

2.1 Changes to the 2011 assessment model of PAU 7

Three changes were made to the 2011 assessment model of PAU 7. One was to allow an annual step change in selectivity, which was estimated in the model to echo the increase of minimum harvest size from 125 mm to 126 mm between Cape Koamaru to Wairau River (see Fu et al. 2016) since 2014–15:

$$V_k^{t,s} = \frac{1}{1+19^{-\left(\left(l_k - D_{50} - D_t^a D^s\right) \Big/ D_{95-50}\right)}}$$

The second change was made so that the predicted CPUE was calculated after 50% of the fishing and natural mortality have occurred (Previously the CPUE indices were fitted to the vulnerable biomass calculated after 50% of the catch was taken). This is considered to be appropriate if the fishing occurs throughout a year (Schnute 1985). The change was recommended by the paua review workshop held in Wellington in March 2015 (Butterworth et al. 2015). Accordingly, mid-season number (and biomass) was calculated after half of the natural mortality and half of the fishing mortality was applied:

$$N_{t+0.5} = N_t \exp(-0.5M)\left(1 - \frac{\left(1 - A_t\right)}{2} V_t^s\right)$$

The third change was made to the likelihood function fitting the tag-recapture observations so that weights can be assigned to individual observations (see Section 2.2.11 for the details). This was also to follow the paua review workshop's recommendation that "the tagging data should be weighted by the relative contribution of average yield from the different areas so that the estimates could better reflect the growth rates from the more productive areas" (Butterworth et al. 2015).

2.2 Model description

The model partitioned the paua stock into a single sex population, with length classes from 70 mm to 170 mm, in groups of 2 mm (i.e., from 70 to under 72 mm, 72 mm to under 74 mm, etc.). The largest length bin is a plus group. An exploratory run was conducted to examine the effect of starting the length class from 2 mm (see section 3.1). The stock was assumed to reside in a single, homogeneous area. The partition accounted for numbers of paua by length class within an annual cycle, where movement between length classes was determined by the growth parameters. Paua entered the partition following recruitment and were removed by natural mortality and fishing mortality.

The model annual cycle was based on the fishing year. Note that model references to "year" within this paper refer to the fishing year, and are labelled as the most recent calendar year, i.e., the fishing year 1998–99 is referred to as "1999" throughout. References to calendar years are denoted specifically.

The models were run for the years 1965–2015. The model assumes one time step within an annual cycle. Catches were collated for 1974–2015, and were assumed to increase linearly between 1965 and 1973 from 0 to the 1974 catch level. Catches included commercial, recreational, customary, and illegal catch, and all catches occurred at the same time step.

Recruitment was assumed to take place at the beginning of the annual cycle, and length at recruitment was defined by a uniform distribution with a range between 70 and 80 mm. Recruitment deviations were assumed known and equal to 1 for the years up to 1980. This was ten years before the length data were available (loosely based on the approximate time taken for recruited paua to appear at the right hand end of the length distribution). The stock-recruitment relationship is unknown for paua, but is likely to be weak (Shepherd et al. 2001). A relationship may exist on small scales, but may not be apparent when large-scale data are modelled (Breen et al. 2003). This assessment assumed a Beverton-Holt stock-recruitment relationship with a steepness of 0.75 for the base case.

Maturity does not feature in the population partition. The model estimated proportions mature with the inclusion of length-at-maturity data. Growth and natural mortalities were also estimated within the model.

The models used two selectivities: the commercial fishing selectivity and the Fighting Bay catch sample selectivity — both assumed to follow a logistic curve (see later).

The model is implemented in AD Model Builder™ (Otter Research Ltd., http://otter-rsch.com/admodel.htm) version 9.0.65, compiled with the MinGW 4.50 compiler.

The six sets of data collated for the assessment model were: (1) a standardised CPUE series based on CELR data (2) a standardised CPUE series based on PCELR data (3) a commercial catch sampling length frequency series (4) tag-recapture length increment data, (5) maturity-at-length data, and (6) the length frequency from the Fighting Bay fish-down experiment.

2.2.1 Estimated parameters

Parameters estimated by the model are as follows. The parameter vector is referred to collectively as θ.

$\ln(R0)$	natural logarithm of base recruitment
M	instantaneous rate of natural mortality
g_1	expected annual growth increment at length L_1

g_2	expected annual growth increment at length L_2
ϕ	CV of the expected growth increment
α	parameter that defines the variance as a function of growth increment
β	parameter that defines the variance as a function of growth increment
$\Delta_{\max}$	maximum growth increment
l_{50}^{g}	length at which the annual increment is half the maximum
l_{95}^{g}	length at which the annual increment is 95% of the maximum
l_{95-50}^{g}	difference between l_{50}^{g} and l_{95}^{g}
q^{I}	scalar between recruited biomass and CPUE
q^{I_2}	scalar between recruited biomass and PCPUE
L_{50}	length at which maturity is 50%
L_{95-50}	interval between L_{50} and L_{95}
T_{50}	length at which Fighting Bay LF selectivity is 50%
T_{95-50}	difference between T_{50} and T_{95}
D_{50}	length at which commercial diver selectivity is 50%
D_{95-50}	difference between D_{50} and D_{95}
D^{s}	change in commercial diver selectivity for one unit change of MHS
$\tilde{\sigma}$	common component of error
h	shape of CPUE *vs.* biomass relation
ε	vector of annual recruitment deviations, from 1977 to 2013
H	steepness of the Beverton-Holt stock-recruitment relationship

2.2.2 Constants

l_k	length of a paua at the midpoint of the k^{th} length class (l_k for class 1 is 71 mm, for class 2 is 73 mm and so on)
σ_{MIN}	minimum standard deviation of the expected growth increment (assumed to be 1 mm)
σ_{obs}	standard deviation of the observation error around the growth increment (assumed to be 0.25 mm)
MLS_t	minimum legal size in year t (assumed to be 125 mm for all years)
$P_{k,t}$	a switch based on whether abalone in the k^{th} length class in year t are above the minimum legal size (MLS) ($P_{k,t}$ = 1) or below ($P_{k,t}$ = 0)
a, b	constants for the length-weight relation, taken from Schiel & Breen (1991) (2.592E-08 and 3.322 respectively, giving weight in kg)
w_k	the weight of an abalone at length l_k
ϖ^{I}	relative weight assigned to the CPUE dataset. This and the following relative weights were varied between runs to find a basecase with balanced residuals
ϖ^{I2}	relative weight assigned to the PCPUE dataset.
ϖ^{F}	relative weight assigned to FBLF dataset
ϖ^{s}	relative weight assigned to CSLF dataset
ϖ^{mat}	relative weight assigned to maturity-at-length data

ϖ^{tag}	relative weight assigned to tag-recapture data
ϖ_j^{tag}	relative weight assigned to tag-recapture observations that from area *j*
$U^{\max}$	exploitation rate above which a limiting function was invoked (0.80 for the base case)
μ_M	mean of the prior distribution for *M*
σ_M	assumed standard deviation of the prior distribution for *M*
σ_ε	assumed standard deviation of recruitment deviations in log space (part of the prior for recruitment deviations)
n_ε	number of recruitment deviations
L_1	length associated with g_1 (75 mm)
L_2	length associated with g_2 (120 mm)
D_t^a	Change in Minimum Harvest Size (MHS) in year *t*, (exogenous variable associated with the change in commercial diver selectivity in year *t*)

2.2.3 Observations

C_t	observed catch in year *t*
I_t	standardised CPUE in year *t*
$I2_t$	standardised PCPUE in year *t*
σ_t^I	standard deviation of the estimate of observed CPUE in year *t*, obtained from the standardisation model
cv_t^I	CV of the estimate of observed CPUE in year *t*, obtained from the standardisation model
σ_t^{I2}	standard deviation of the estimate of observed PCPUE in year *t*, obtained from the standardisation model
cv_t^{I2}	CV of the estimate of observed PCPUE in year *t*, obtained from the standardisation model
p_k^F	observed proportion in the k^{th} length class in FDLF
$p_{k,t}^s$	observed proportion in the k^{th} length class in year *t* in CSLF
l_j	initial length for the j^{th} tag-recapture record
d_j	observed length increment of the j^{th} tag-recapture record
Δt_j	time at liberty for the j^{th} tag-recapture record
p_k^{mat}	observed proportion mature in the k^{th} length class in the maturity dataset

2.2.4 Derived variables

R0	base number of annual recruits
$N_{k,t}$	number of paua in the k^{th} length class at the start of year *t*
$N_{k,t+0.5}$	number of paua in the k^{th} length class in the mid-season of year *t*
$R_{k,t}$	recruits to the model in the k^{th} length class in year *t*
g_k	expected annual growth increment for paua in the k^{th} length class
σ^{g_k}	standard deviation of the expected growth increment for paua in the k^{th} length class, used in calculating $\mathbf{G}$
$\mathbf{G}$	growth transition matrix

B_t	spawning stock biomass at the beginning of year *t*
$B_{t+0.5}$	spawning stock biomass in the mid-season of year *t*
B_0	equilibrium spawning stock biomass assuming no fishing and average recruitment from the period in which recruitment deviations were estimated.
B_t^r	biomass of paua above the MLS at the beginning of year *t*
$B_{t+0.5}^r$	biomass of paua above the MLS in the mid-season of year *t*
B_0^r	equilibrium biomass of paua above the MLS assuming no fishing and average recruitment from the period in which recruitment deviations were estimated
B_t^v	available (to commercial fishing) biomass of paua at the beginning of year *t*
U_t	exploitation rate in year *t*
A_t	the complement of exploitation rate
$SF_{k,t}$	finite rate of survival from fishing for paua in the k^{th} length class in year *t*
V_k^F	relative selectivity of Fighting Bay LF for paua in the k^{th} length class
V_k^s	relative selectivity of commercial divers for paua in the k^{th} length class
σ_k^r	error of the predicted proportion in the k^{th} length class in year *t* in FBLF data
n^r	relative weight (effective sample size) of the FBLF data in year *t*
$\sigma_{k,t}^s$	error of the predicted proportion in the k^{th} length class in year *t* in CSLF data
n_t^s	relative weight (effective sample size)of the CSLF data in year *t*
σ_j^d	standard deviation of the predicted length increment for the j^{th} tag-recapture record
σ_j^{tag}	total error predicted for the j^{th} tag-recapture record
σ_k^{mat}	error of the proportion mature-at-length for the k^{th} length class
$-\ln(\mathbf{L})$	negative log-likelihood
f	total function value

2.2.5 Predictions

$\hat{I}_t$	predicted CPUE in year *t*
$\hat{I}2_t$	predicted PCPUE in year *t*
$\hat{p}_{k,1965}^r$	predicted proportion in the k^{th} length class in Fighting Bay LF (assumed representing the population LF in year 1965)
$\hat{p}_{k,t}^s$	predicted proportion in the k^{th} length class in year *t* in commercial catch sampling
$\hat{d}_j$	predicted length increment of the j^{th} tag-recapture record
$\hat{p}_k^{mat}$	predicted proportion mature in the k^{th} length class

2.2.6 Initial conditions

The initial population is assumed to be in equilibrium with zero fishing mortality and the base recruitment. The model is run for 60 years with no fishing to obtain near-equilibrium in numbers-at-length. Recruitment is evenly divided among the first five length bins:

(1) $R_{k,t} = 0.2R0 \qquad \text{for } 1 \le k \le 5$

(2) $R_{k,t} = 0 \qquad \text{for } k > 5$

A growth transition matrix is calculated inside the model from the estimated growth parameters. The base case used the inverse-logistic model, and the expected annual growth increment for the k^{th} length class is:

(3) $$\Delta l_k = \frac{\Delta_{\max}}{\left(1+\exp\left(\ln(19)\left(\left(l_k - l^g_{50}\right)/\left(l^g_{95} - l^g_{50}\right)\right)\right)\right)}$$

If the growth model is exponential, the expected annual growth increment for the k^{th} length class is:

(4) $$\Delta l_k = g_1\left(g_2 / g_1\right)^{(l_k - L_1)/(L_2 - L_1)}$$

If the growth model is linear, the expected annual growth increment for the k^{th} length class is:

(5) $$\Delta l_k = \left(\frac{L_2 g_1 - L_1 g_2}{g_1 - g_2} - l_k\right)\left[1 - \left(1 + \frac{g_1 - g_2}{L_1 - L_2}\right)\right]$$

The model uses the AD Model Builder™ function *posfun*, with a dummy penalty, to ensure a positive expected increment at all lengths, using a smooth differentiable function.

All the models were examined and the logistic growth model was chosen for fitting the tag-recapture data in the base case of the PAU 7 assessment.

The standard deviation of g_k is assumed to be proportional to g_k with minimum σ_{MIN}:

(6) $$\sigma^{g_k} = \left(g_k\phi - \sigma_{MIN}\right)\left(\frac{1}{\pi}\tan^{-1}\left(10^6\left(g_k\phi - \sigma_{MIN}\right)\right) + 0.5\right) + \sigma_{MIN}$$

Or a more complex functional form between the growth increment and its standard deviation can be defined as:

(7) $$\sigma^{g_k} = \left(\alpha\left(g_k\right)^{\beta} - \sigma_{MIN}\right)\left(\frac{1}{\pi}\tan^{-1}\left(10^6\left(\alpha\left(g_k\right)^{\beta} - \sigma_{MIN}\right)\right) + 0.5\right) + \sigma_{MIN}$$

From the expected increment and standard deviation for each length class, the probability distribution of growth increments for a paua of length l_k is calculated from the normal distribution and translated into the vector of probabilities of transition from the k^{th} length bin to other length bins to form the growth transition matrix **G**. Zero and negative growth increments are permitted, i.e., the probability of staying in the same bin or moving to a smaller bin can be non-zero.

In the initialisation, the vector $\mathbf{N_t}$ of numbers-at-length is determined from numbers in the previous year, survival from natural mortality, the growth transition matrix **G,** and the vector of recruitment $\mathbf{R_t}$:

(8) $$\mathbf{N_t} = \left(\mathbf{N_{t\text{-}1}}\, e^{-M}\right) \bullet \mathbf{G} + \mathbf{R_t}$$

where the dot (•) denotes matrix multiplication.

2.2.7 Dynamics

2.2.7.1 Sequence of operations

After initialising, the first model year is 1965 and the model is run through to 2015. In the first nine years the model is run with an assumed catch vector, because it is unrealistic to assume that the fishery was in a virgin state when the first catch data became available in 1974. The assumed catch vector rises linearly from zero to the 1974 catch. These years can be thought of as an additional part of the initialisation, but they use the dynamics described in this section.

Model dynamics are sequenced as follows.

- Numbers at the beginning of year *t*-1 are subjected to fishing, then natural mortality, then growth to produce the numbers at the beginning of year *t*.
- Recruitment is added to the numbers at the beginning of year *t*.
- Biomass available to the fishery is calculated and, with catch, is used to calculate the exploitation rate, which is constrained if necessary.
- Half the exploitation rate and half natural mortality is applied to obtain mid-season numbers, from which the predicted abundance indices and proportions-at-length are calculated. Mid-season numbers are not used further.

2.2.7.2 Main dynamics

For each year *t*, the model calculates the start-of-the-year biomass available to the commercial fishery. Biomass available to the commercial fishery is:

(9) $$B_t^v = \sum_k N_{k,t} V_k^s w_k$$

(10) $$V_k^{t,s} = \frac{1}{1+19^{-\left(\left(l_k - D_{50}\right)/D_{95-50}\right)}} \qquad \text{for } t < 2015$$

(11) $$V_k^{t,s} = \frac{1}{1+19^{-\left(\left(l_k - D_{50} - D_t^a D^s\right)/D_{95-50}\right)}} \qquad \text{for } t \geq 2015$$

The observed catch is then used to calculate the exploitation rate, constrained for all values above U^{max} with the *posfun* function of AD Model Builder™. If the ratio of catch to available biomass

exceeds U^{max}, then exploitation rate is constrained and a penalty is added to the total negative log-likelihood function. Let minimum survival rate A_{min} be 1-U^{max} and survival rate A_t be 1-U_t:

(12) $$A_t = 1 - \frac{C_t}{B_t^v} \quad \text{for} \quad \frac{C_t}{B_t^v} \le U^{\max}$$

(13) $$A_t = 0.5A_{\min}\left[1 + \left(3 - \frac{2\left(1 - \frac{C_t}{B_t^v}\right)^{-1}}{A_{\min}}\right)\right] \quad \text{for} \quad \frac{C_t}{B_t^v} > U^{\max}$$

The penalty invoked when the exploitation rate exceeds U^{max} is:

(14) $$10000000\left(A_{\min} - \left(1 - \frac{C_t}{B_t^r}\right)\right)^2$$

This prevents the model from exploring parameter combinations that give unrealistically high exploitation rates. Survival from fishing is calculated as:

(15) $$SF_{k,t} = 1 - (1 - A_t)P_{k,t}$$

or

(16) $$SF_{k,t} = 1 - (1 - A_t)V_k^s$$

The vector of numbers-at-length in year *t* is calculated from numbers in the previous year:

(17) $$\mathbf{N_t} = \left(\left(\mathbf{SF_{t\text{-}1}} \otimes \mathbf{N_{t\text{-}1}}\right)\mathrm{e}^{-M}\right) \bullet \mathbf{G} + \mathbf{R_t}$$

where $\otimes$ denotes the element-by-element vector product. The vector of recruitment, $\mathbf{R_t}$, is determined from *R0*, estimated recruitment deviations, and the stock-recruitment relationship:

(18) $$R_{k,t} = 0.2R0e^{\left(\varepsilon_t - 0.5\sigma_t^2\right)} \frac{B_{t-1+0.5}}{B_0} \Big/ \left(1 - \frac{5H-1}{4H}\left(1 - \frac{B_{t-1+0.5}}{B_0}\right)\right) \quad \text{for} \quad 1 \le k \le 5$$

(19) $$R_{k,t} = 0 \quad \text{for} \quad k > 5$$

The recruitment deviation parameters ε_t were estimated for all years from 1980. The recruitment deviations were constrained to have a mean of 1 in arithmetic space.

The model predicts CPUE in year *t* from mid-season recruited biomass, the scaling coefficient, and the shape parameter:

(20) $$\hat{I}_t = q^I \left(B_{t+0.5}^v\right)^h$$

Available biomass $B_{t+0.5}^v$ is the mid-season vulnerable biomass after half the catch has been removed and half natural mortality is applied (because the catch occurred throughout the fishing year). It is

calculated as in equation **Error! Reference source not found.**, but using the mid-year numbers, $N_{k,t+0.5}$:

$$N_{t+0.5} = N_t \exp(-0.5M)\left(1 - \frac{(1-A_t)}{2} V_t^s\right). \quad (21)$$

Similarly,

$$\hat{I}2_t = q^{I2}\left(B^v_{t+0.5}\right)^h \quad (22)$$

The same shape parameter *h* is used for both the early and recent CPUE series.
The Fighting Bay LF selectivity V_k^r is calculated from:

$$V_k^F = \frac{1}{1+19^{-\left((l_k - T_{50})/T_{95-50}\right)}} \quad (23)$$

The model predicts proportions-at-length for the CSLF from numbers in each length class for lengths greater than 116 mm:

$$\hat{p}^s_{k,t} = \frac{N_{k,t+0.5} V^s_{k,t}}{\sum_{k=23}^{51} N_{k,t+0.5} V^s_{k,t}} \qquad \text{for } 23 \le k < 51 \quad (24)$$

Predicted proportions-at-length for FBLF are similar:

$$\hat{p}^F_{k,1965} = \frac{N_{k,t+0.5} V^F_k}{\sum_{k=25}^{51} N_{k,t+0.5} V^F_k} \qquad \text{for } 25 \le k \le 51 \text{ and } t = 1965 \quad (25)$$

The predicted increment for the j^{th} tag-recapture record, using the inverse-logistic model, is:

$$\hat{d}_j = \frac{\Delta_{\max}}{\left(1+\exp\left(\ln(19)\left(\left(l_j - l^g_{50}\right)/\left(l^g_{95} - l^g_{50}\right)\right)\right)\right)} \quad (26)$$

For the exponential model () the expected increment is

$$\hat{d}_j = \Delta t_j g_\alpha \left(g_\beta / g_\alpha\right)^{(L_j - \alpha)/(\beta - \alpha)} \quad (27)$$

where Δt_j is in years. The error around an expected increment is:

$$\sigma_j^{\,d} = \left(\hat{d}_j \phi - \sigma_{MIN}\right)\left(\frac{1}{\pi}\tan^{-1}\left(10^6\left(\hat{d}_j \phi - \sigma_{MIN}\right)\right) + 0.5\right) + \sigma_{MIN} \quad (28)$$

Predicted maturity-at-length is:

(29) $$\hat{p}_k^{mat} = \frac{1}{1+19^{-\left((l_k - L_{50})/L_{95-50}\right)}}$$

2.2.8 Fitting

2.2.8.1 Likelihoods

The distribution of CPUE is assumed to be normal-log and the negative log-likelihood is:

(30) $$-\ln(\mathbf{L})\left(\hat{I}_t \mid \theta\right) = \frac{\left(\ln\left(I_t\right) - \ln\left(\hat{I}_t\right)\right)^2}{2\left(\sigma_t^I \tilde{\sigma} / \varpi^I\right)^2} + \ln\left(\sigma_t^I \tilde{\sigma} / \varpi^I\right) + 0.5\ln\left(2\pi\right)$$

Where

(31) $$\sigma_t^I = \sqrt{\log((cv_t^I)^2 + 1)}$$

and similarly for PCPUE:

(32) $$-\ln(\mathbf{L})\left(\hat{I}2_t \mid \theta\right) = \frac{\left(\ln\left(I2_t\right) - \ln\left(\hat{I}2_t\right)\right)^2}{2\left(\sigma_t^{I2} \tilde{\sigma} / \varpi^{I2}\right)^2} + \ln\left(\sigma_t^{I2} \tilde{\sigma} / \varpi^{I2}\right) + 0.5\ln\left(2\pi\right)$$

Where

(33) $$\sigma_t^{I2} = \sqrt{\log((cv_t^{I2})^2 + 1)}$$

The proportions-at-length from CSLF data are assumed to follow a multinomial distribution, with a standard deviation that depends on the effective sample size (see Section 2.2.9.3) and the weight assigned to the data:

(34) $$\sigma_{k,t}^s = \frac{\tilde{\sigma}}{\varpi^s n_t^s}$$

The negative log-likelihood is:

(35) $$-\ln(\mathrm{L})\left(\hat{p}_{k,t}^s \mid \theta\right) = \frac{p_{s,t}^s}{\sigma_{k,t}^s}\left(\ln\left(p_{k,t}^s + 0.01\right) - \ln\left(\hat{p}_{k,t}^s + 0.01\right)\right)$$

The likelihood for Fighting Bay LF is analogous. Errors in the tag-recapture dataset were also assumed to be normal. For the j^{th} record, the total error is a function of the predicted standard deviation (equation (28)), observation error, and weight assigned to the data:

(36) $$\sigma_j^{tag} = \tilde{\sigma} / \varpi^{tag} \sqrt{{\sigma_{obs}}^2 + \left(\sigma_j^d\right)^2}$$

The negative log-likelihood for an observation is:

$$-\ln(L)\left(\hat{d}_j \mid \theta\right) = \omega_g^{tag}\left(\frac{\left(d_j - \hat{d}_j\right)^2}{2\left(\sigma_j^{tag}\right)^2} + \ln\left(\sigma_j^{tag}\right)^2 + 0.5\ln(2\pi)\right) \quad (37)$$

where ω_g^{tag} is an weighing factor calculated as

$$\omega_g^{tag} = p_g \frac{\sum_g n_g}{n_g} \quad (38)$$

where p_g is the proportion of catch from area g (where the observation is made), and n_g is the number of tag-recapture observations from area g. This allows the likelihood to be influenced by the catch proportion of each area, but not the size of observations. ω_g^{tag} can be fixed at 1 if the likelihood is not to be weighted.

The proportion mature-at-length was assumed to be normally distributed, with standard deviation analogous to proportions-at-length:

$$\sigma_k^{mat} = \frac{\tilde{\sigma}}{\varpi^{mat}\sqrt{p_k^{mat} + 0.1}} \quad (39)$$

The negative log-likelihood is:

$$-\ln(\mathbf{L})\left(\hat{p}_k^{mat} \mid \theta\right) = \frac{\left(p_k^{mat} - \hat{p}_k^{mat}\right)^2}{2\left(\sigma_k^{mat}\right)^2} + \ln\left(\sigma_k^{mat}\right) + 0.5\ln\left(2\pi\right) \quad (40)$$

2.2.8.2 Normalised residuals

These are calculated as the residual divided by the relevant σ term used in the likelihood. For CPUE, the normalised residual is

$$\frac{\ln\left(I_t\right) - \ln\left(\hat{I}_t\right)}{\left(\sigma_t^I \tilde{\sigma} \Big/ \varpi^I\right)} \quad (41)$$

and similarly for PCPUE. For the CSLF proportions-at-length, the residual is:

$$\frac{p_{k,t}^s - \hat{p}_{k,t}^s}{\sigma_{k,t}^s} \quad (42)$$

and similarly for proportions-at-length from the FBLF.

For tag-recapture data, the residual is:

$$\frac{d_j - \hat{d}_j}{\sigma_j^{tag}} \quad (43)$$

and for the maturity-at-length data the residual is:

$$\frac{p_k^{mat} - \hat{p}_k^{mat}}{\sigma_k^{mat}} \quad (44)$$

2.2.8.3 Dataset weights

Proportions at length (CSLF and FBLF) were included in the model with a multinomial likelihood. The length frequencies for individual years were assigned relative weights (effective sample size), based on a sample size that represented the best least squares fit of log(cv_i)~log(P_i), where cv_i was the bootstrap CV for the ith proportion, P_i. (See Figure A1, Appendix A, for a plot of this relationship). The weights for individual years (n_t^s for CSLF and n_t^F for FBLF) were multiplied by the weight assigned to the dataset (ϖ^s for CSLF and ϖ^F for FBLF) to obtain the model weights for the observations. We used the weighting scheme following Francis (2012) for the base case model, where the weight for the CSLF dataset was determined as

$$\varpi^s = 1/\operatorname{var}_t\left[\left(\overline{O}_t^s - \overline{E}_t^s\right)/\left(v_t^s / n_t^s\right)^{0.5}\right] \quad \text{(Method TA1.8, table A1 in Francis 2011)} \quad (45)$$

Where

$$\overline{O}_t^s = \sum_k p_{k,t}^s l_k \quad (46)$$

$$\overline{E}_t^s = \sum_k \hat{p}_{k,t}^s l_k \quad (47)$$

$$v_t^s = \sum_k \left(l_k\right)^2 \hat{p}_{k,t}^s - \left(\overline{E}_t^s\right)^2 \quad (48)$$

The Fighting Bay length frequency was assumed to represent the initial state of the population (in 1965) and the sample size was simply fixed to be 100 (TA1.8 method requires at least a few years of data). The TA1.8 method allows for the possibility of substantial correlations within a dataset, and generally produces relatively smaller sample sizes, thus down-weighting the composition data (Francis 2011). Alternatively an iterative reweighting approach by McAllister & Ianelli (1997) was considered. This approach assumes a single effective sample size for all years and adjusts it iteratively so the expected variances from model predictions matches observed variance (see McAllister & Ianelli (1997) for details). The McAllister & Ianelli (1997) weighting approach was only used in one of the preliminary trials. The actual and estimated sample sizes for the commercial catch at length using the two methods are given in Table 1.

The relative abundance indices (CPUE and PCPUE) were included in the model with a lognormal likelihood. The weights for individual years were determined by the CV calculated in the standardisation and were then scaled by the weight assigned to the dataset to obtain the model weights for the observations. In previous assessments, the weight of the dataset was determined iteratively so that the standard deviation of the normalised residuals was close to one. In this assessment, we used a weighting scheme recommended by Francis (2011), with a small modification recommended by the review workshop (Butterworth et al. 2015). With this approach, a series of lowess lines of various degrees of smoothing were fitted to the abundance indices (this was carried out outside the assessment model), and the CV was calculated using the residuals from the lowess line which is considered to have the "appropriate" smoothness. This CV was then adjusted for the degrees of freedom associated with the smoothing:

$$cv' = cv\left(\frac{n}{n-d}\right) \quad (49)$$

Where cv was calculated using the residuals, n is the number of indices, d is degree of freedom, and cv' was the adjusted value. The adjusted CV was applied to all years in the time series and remained constant in the stock assessment model. The choice of the "appropriate" fit was based on visual examination of the lowess lines. This is equivalent to saying that we expect the stock assessment model to fit these data as well as the smoother.

For the early CPUE (1990–2001), the residuals from the lowess line which has the "appropriate" smoothness (*df*=5) have an adjusted CV of 0.1 (Figure A2–left, Appendix A); for the recent CPUE (2002–2015), a CV of 0.08 was considered to be appropriate (*df*=5, Figure A2–right, Appendix A). The CVs of the CPUE observations in the assessment model were fixed at those values (except for sensitivity run 1.1 and 1.2 in which alterative values were used)

2.2.8.4 Priors and bounds

Bayesian priors were established for all estimated parameters (Table 2). Most were incorporated simply as uniform distributions with upper and lower bounds set arbitrarily wide so as not to constrain the estimation. The prior probability density for M was a normal-log distribution with mean μ_M and standard deviation σ_M. The contribution to the objective function of estimated $M = x$ is:

$$-\ln(\mathbf{L})(x \mid \mu_M, \sigma_M) = \frac{\left(\ln(M) - \ln(\mu_M)\right)^2}{2\sigma_M{}^2} + \ln\left(\sigma_M \sqrt{2\pi}\right) \quad (50)$$

The prior probability density for the vector of estimated recruitment deviations ε, was assumed to be normal with a mean of zero and a standard deviation of 0.4. The contribution to the objective function for the whole vector is:

$$-\ln(\mathbf{L})(\varepsilon \mid \mu_\varepsilon, \sigma_\varepsilon) = \frac{\sum_{i=1}^{n_\varepsilon} (\varepsilon_i)^2}{2\sigma_\varepsilon{}^2} + \ln(\sigma_\varepsilon) + 0.5\ln(2\pi). \quad (51)$$

Constant parameters are given in Table 3

2.2.8.5 Penalty

A penalty is applied to exploitation rates higher than the assumed maximum (equation 13). The penalty is added to the objective function after being multiplied by an arbitrary weight (1000000) determined by experiment.

AD Model Builder™ also has internal penalties that keep estimated parameters within their specified bounds, but these should have no effect on the final outcome, because choice of a base case excludes the situations where parameters are estimated at or near a bound.

2.2.9 Fishery indicators

The assessment calculates the following quantities from their posterior distributions: the model's mid-season spawning and recruited biomass for 2015 ($B_{current}$ and $B^r_{current}$) and for the projection period (B_{proj} and B^r_{proj}).

Simulations were carried out to calculate deterministic MSY: maximum constant annual catch that can be sustained under deterministic recruitment. A single simulation run was done by starting from

an unfished equilibrium state, and running under a constant exploitation rate until the catch and spawning stock biomass stabilised. For each simulation run with exploitation rate *U*, the equilibrium total annual catch and spawning stock biomass were calculated. The exploitation rate *U* that maximizes the annual catch is U_{msy}. The corresponding catch is MSY, and the corresponding SSB is B_{msy}. Together with B_o, B_{msy}, $U_{current}$, $U_{\%40B0}$ and U_{msy} the current and projected stock status is reported in relation to the following indicators:

$\%B_0$	current and projected spawning biomass as a percent of B_0
$\%B_{msy}$	current and projected spawning biomass as a percent of B_{msy}
$\Pr(> B_{current})$	Probability that projected spawning biomass is greater than $B_{current}$
$\Pr(> B_{msy})$	Probability that current and projected spawning biomass is greater than B_{msy}
$\%B_0^r$	current and projected recruited biomass as a percent of B_0^r
$\%B_{msy}^r$	current and projected recruited biomass as a percent of B_{msy}^r
$\Pr(> B_{msy}^r)$	Probability that current and projected recruit-sized biomass is greater than B_{msy}^r
$\Pr(> B_{current}^r)$	Probability that projected recruit-sized biomass is greater than $B_{current}^r$
$\Pr(B_{proj} > 40\%B_0)$	Probability that current and projected spawning biomass is greater than 40% B_0
$\Pr(B_{proj} < 20\%B_{msy})$	Probability that current and projected spawning biomass is less than 20% B_0
$\Pr(B_{proj} < 10\%B_{msy})$	Probability that current and projected spawning biomass is less than 10% B_0
$\Pr(U_{proj} > U_{40\%B0})$	Probability that current and projected exploitation rate is greater than $U_{40\%B0}$

2.2.10 Markov chain-Monte Carlo (MCMC) procedures

AD Model Builder™ uses the Metropolis-Hastings algorithm. The step size is based on the standard errors of the parameters and their covariance relationships, estimated from the Hessian matrix.

For the MCMCs in this assessment single long chains were run, starting at the MPD estimate. The base case was 5 million simulations long and samples were saved, regularly spaced by 5000. The value of $\tilde{\sigma}$ was fixed to that used in the MPD run because it may be inappropriate to let a variance component change during the MCMC.

2.2.11 Development of base case and sensitivity model runs

Following discussions of input data by the Shellfish Working Group (SFWG), an ensemble of initial model runs were conducted. The initial models investigated aspects of model configurations, weighting methods, choice of growth models, inclusion of alternative CPUE indices and catch histories. The configurations of the initial model runs are summarised in Table A.1, Appendix A. Changes between these models were made in a sequential manner so that the effects of those differences to model estimates can be assessed. The results of the initial model runs are briefly summarised in Section 3.1.

After reviewing the diagnostics and outputs from the initial models, the Shellfish WG agreed on a base case (1.0). The base case model is configured such that (a) predicted CPUE is calculated after half of the natural and fishing mortality has occurred; (b) Francis (2012) method was used to determine the weight of CSLF and CPUE; (c) growth was estimated using the inverse-logistic model;

(d) FBLF was included in the model; (e) tag-recapture observations from the Staircase were excluded; (f) tag-recapture observations were weighted by the catch in each area; (g) negative growth was permitted in the growth transition matrix; (h) the CPUE shape parameter was fixed at 1 assuming a linear relationship between CPUE and abundance.

The SFWG also suggested the following sensitivity runs: using a smaller CV of 0.05 (model 1.1), or a larger CV of 0.12 (1.2); estimating the CPUE shape parameter assuming a uniform prior bounded between 0.5 and 1.5 (1.3), or fixing it at the lower (1.3a) and upper value (1.3b) respectively; using an alternative prior when estimating natural mortality (1.4, see below); including tag-recapture observations from the Staircase (1.5). A description of the base case and sensitivity models is given in Table 4.

The base case used a lognormal prior on M, with μ_M = 0.1 and σ_M =0.1. The mean was based on a literature review by Shepherd & Breen (1992). The choice of CV was arbitrary, but generally chosen to be very informative to prevent obtaining unrealistic estimates. The paua review workshop (Butterworth et al. 2015) has recommended a procedure to develop a prior using information from assessment of other QMA stocks. A slightly modified version of that procedure was implemented as below:

(i) Re-run the base case of most recent assessments for each QMA, using an uninformative prior U [0.05; 0.25] for M.
(ii) Review the posteriors for M for each assessment, and determine the QMAs in which the prior for M is meaningfully updated. The associated posteriors are considered to provide the best estimate of M for those QMAs.
(iii) Estimate the mean and standard deviations from the combined posterior samples of M from QMAs chosen from step 2 (using a lognormal distribution), and increase the standard deviation by 50% to provide a broadened distribution.
(iv) Use the mean and standard deviation obtained from step (iii) as the prior.

3. RESULTS

3.1 Preliminary model runs

Diagnostics from preliminary models runs (0.1–0.13) are given in Appendix A (Table A.1, Figures A3-A13). Key conclusions drawn from these diagnostics are summarised below.

- Assuming that half of the fishing and natural mortality had occurred when calculating CPUE fits, appeared to have no effect on the predicted values, but resulted in slightly higher biomass estimates overall (Figure A3).

- The inverse-logistic growth model was considered to be better than the exponential model in this case based on the likelihood value of the fits to the growth data and residual patterns (Figure A4).

- Removing tag-recapture observations from the Staircase resulted in a small increase in estimated growth rates, especially for the smaller size classes below the minimum harvest size (Figure A5). There is also a noticeable improvement in residual patterns (Figure A5).

- Variation of mean growth was estimated to be smaller when tag-recapture observations from the Staircase were excluded. This had little effect on the equilibrium population length structure if initial recruitment (into the population) was assumed to occur at 70 mm (Figure A6, top left). Extending the partition to 2 mm allowed the model to better capture any cohort effect across smaller size classes, but did not change the estimated biomass (Figure A6, top right and bottom graphs).

- The assessment model permits paua to transition from large to smaller size classes (because the distribution of growth increment at length could fall below zero). Negative growth is not permitted in some assessment tools (e.g. CASAL (Bull et al. 2012)). The exploratory run in which the growth transition matrix was adjusted so that it does not permit negative growth found that this has almost no effect on results (Figure A7).

- Weighting tag-recapture observations by the catch resulted in higher estimates of mean growth because areas in which paua grow fast (e.g. Runder and Perano) accounted for most of the catch. The biomass estimates were lower than in the model in which equal weights were assigned to individual observations (Figure A8).

- Including the Fighting Bay length frequency did not change the estimate of growth rates, and this dataset was fitted well (Figure A9).

- Using the McAllister & Ianelli (1997) method produced larger sample sizes for CSLF than the Francis (2012) method, but it made little difference to the fits to the CSLF or biomass estimates (Figure A10).

- Using an alternative commercial catch history for 1981–1983 (see Fu et al. 2016) only had a small effect on biomass estimates before 1980 (Figure A11).

- The PCPUE indices developed by Neubauer (2015), which incorporated spatial-temporal correlations, suggested that the biomass increased in 2014 and 2015 (Figure A12). The combined CELR/PCELR standardised indices (Fu et al. 2016) suggested that the decline in abundance between 1990 and 2015 was much less than what was estimated in the model when separate indices were used. (Figure A13).

3.2 MPD base case and sensitivity

MPD estimates of objective function values (negative log-likelihood), parameters, and indicators for the base case and sensitivities are summarised in Table 5. The base case model matched very closely with the early CPUE and predicted CPUE indices were all well within the confidence bounds of the observed values (Figure 2). Predicted CPUE declined more than observed values between 2009 and 2013. However, the overall change in relative abundance between 2002 and 2015 is similar between the predicted and observed values. The standardised residuals show no apparent departure of the model's assumption of normality (Figure 3). Commercial catch length frequencies were well fitted for most years (Figure 4). The mean length of CSLF has increased since 2003, and has remained reasonably stable since 2007, except in 2014 (Figure 5–left). The average fish size in the catch in recent years has been well below those in the early 1990s (Figure 5–left). The standardised residuals of the fits to CSLF revealed that in general the model predicted a slightly narrower distribution than what was observed in the catch (Figure 5–right). This might be because the population has been fished down to a low level and the chance of sampling paua of large sizes was reduced. Estimated logistic selectivity was very close to knife-edge around the MLS, with a small increase in 2015 (Table 5). Fits to growth increment and maturity data appeared adequate (Figure 6). The relative weight assigned to tag-recapture observations from Perano and Runder was about three times more than those from Northern Faces, and as a result, estimated mean growth was higher than if equal weights were assumed (see Section 3.1 and Figure A8). The Fighting Bay length frequency was fitted well (Figure 7), suggesting that this length distribution was consistent with the estimated growth rates in the model.

Sensitivity run 1.1 assumed a CV of 5% for recent CPUE indices and fitted this dataset better (Figure 8); sensitivity run 1.2 assumed a CV of 12% and estimated a much steeper decline between 2009 and

2013 than the base case (Figure 8). This appeared to have been driven by the low mean length in 2014 (CSLF was relatively up-weighted when a larger CV was assumed for CPUE indices, Figure 9–left). The reduced mean length in 2014 is unlikely to be explained by sampling variations as this pattern persists across most statistical areas (Figure 9–right). The trend in CSLF suggested that the abundance has declined more than what was observed in the CPUE indices.

The base case fixed the CPUE shape parameter at 1, assuming a linear relationship between CPUE and abundance. Under this assumption, the model estimated that the vulnerable biomass decreased by 47% between 1990 and 2001, and increased by 20% between 2002 and 2015. The CPUE shape parameter (*h*) was estimated to be 1.1 in sensitivity run 1.3, implying a hyper-depleted relationship. However, a profile likelihood analysis showed that CSLF and CPUE had conflicting information regarding this parameter and the estimate was likely to be a mere compromise. Therefore the assumption regarding the relationship between CPUE and abundance could be better assessed by fixing *h* to a low value of 0.5 (hyperstable) or to a high value of 1.5 (hyperdepletion), as recommended by Butterworth et al. (2015). Assuming an *h* of 0.5, the model estimated that the biomass decreased by 58% between 1990 and 2001, and increased by 40% between 2002 and 2015; assuming an *h* of 1.5, the biomass decreased by 40% between 1990 and 2001, and increased by 13% between 2002 and 2015 (Figure 10).

The MPD estimate of natural mortality (M) was 0.12 for the base case. A slightly higher M was estimated for MPD 1.4 which used a lognormal prior of a higher mean (see Section 3.3). The MPD estimate of $B_{current}$ was 17% of B_0 for the base case (model 1.0), and ranged between 16% and 21% for all the sensitivity trials considered (Table 5).

3.3 MCMC results

MCMC was conducted for the base case (1.0), 1.1, 1.2, 1.3, 1.4, and 1.5 to derive the posterior distributions of estimated parameters and biomass indicators.

For sensitivity 1.4, the prior for M was developed using the procedure described in section 2.2.1. Using the base case from the 2015 assessment of PAU 5A south and the 2013 assessment of PAU 5B obtained meaningful updates of M when a uniform prior was used, and in both cases the posterior of M had a much broader distribution with a higher mean than the original estimates (Figure B1, Appendix B). The combined posterior samples (PAU 5A south and PAU 5B) had a mean of 0.15 and a CV of 17%. Based on this result, a lognormal prior with a mean of 0.15 and a CV of 25% was assumed for M in sensitivity 1.4.

3.3.1 Marginal posterior distributions and the Bayesian fit

The traces plot of the posterior samples was used as the main diagnostic for the MCMC. The traces of estimated parameters from the base case show good mixing (Figure 11–left). The traces of key indicators (B_0 and $B_{current}$) show no evidence of non-convergence of the sensitivity models although posterior samples from MCMC 1.4 exhibit some instability partway through the traces (Figure 11–right).

For the base case, estimated recent recruitment has been below average (recruitment in 2010 and 2011 was the lowest after 2002, Figure 12–left). The estimated exploitation rate has declined since 2003, and was further reduced after 2012 (Figure 12–right). The exploitation rate in 2015 was estimated to be 0.46 (0.40–0.52).

Estimated spawning stock biomass (SSB) for the base case is shown in Figure 13: Posterior distributions of spawning stock biomass and spawning stock biomass as a percentage of virgin level from MCMC 1.0. The box shows the median of the posterior distribution (horizontal bar), the 25th and 75th percentiles (box), with the whiskers representing the full range of the distribution.Figure 13 The SSB decreased after 2009 through to 2013, but increased in the last two years. Estimated B_0 was 4291 t (3 980–4 584 t) and $B_{current}$ was 18% (16–21%) of B_0, or 69% (59–81%) of B_{msy} (Table 6). Changes in stock size in response to fishing pressure over time are shown in Figure 14. This was done by plotting the annual spawning biomass and exploitation rate as a ratio of a reference value from 1965 to 2015. Each point on the trajectory represents the estimated annual stock status: the value on the x axis is the mid-season spawning stock biomass as a ratio of either B_0 (Figure 14–left) or B_{msy} (Figure 14–right), the value on the y axis is the corresponding exploitation rate as a ratio of $U_{40\%B0}$ (Figure 14–left) or U_{msy} (Figure 14–right) for that year. The trajectory started in 1965 when the SSB is close to B_0 and the exploitation rate is close to 0. The model indicated an early phase of the fishery where the exploitation rates were below $U_{40\%B0}$ and the SSBs were above 40% B_0 and a development phase where the exploitation rates increased and the SSBs decreased in relation to the target. The current exploitation rate is about twice of $U_{40\%B0}$ and the current spawning stock biomass is just below 20% B_0.

For MCMC 1.1 and 1.2, posterior distributions of the predicted CPUE indices were broadly in keeping with the error assumptions made for the observations (Figure 15). Despite a different CV being assumed for the CPUE, estimates of stock status from these two models were similar to the base case. The CV for CPUE appeared to have more influence on the estimate of catchability q (Figure 16–left), with less influence on the estimated uncertainty of stock status (Figure 16–right).

For MCMC 1.3, the estimated CPUE shape parameter had a broad posterior distribution (Figure 17–left), with a median of 0.84 (much smaller than the MPD estimate). This probably suggests that the available data in the current model were not very informative for this parameter. Estimated stock status was similar to the base case (Figure 17–right).

For MCMC 1.4, estimated M had a much broader posterior than the base case (Figure 18–left), as a result of a less informative prior. Estimated current stock status was higher than the base case, with more uncertainty (Figure 18–right).

For MCMC 1.5, estimated mean growth rates were lower than the base case, especially for the smaller size classes. This sensitivity run resulted a more optimistic estimate of current stock status (Figure 19).

Estimates of biomass trajectories for all model runs are shown in Figure 20. The median of current stock status was below 20% of B_0 for MCMC 1.0, 1.1, 1.2, and 1.3, and was above 20% for MCMC 1.4 and 1.5.

3.3.2 Projections

Forward projections (2016–2018) were made for the base case with a number of alternative future catch scenarios. Future recruitment deviations were resampled from model estimates either from 2002–2011 (a period with both high and low recruitment), or from 2010–2011 (a period with low recruitment). Recruitment randomisations started from 2012 (Figure C1, Appendix C). When recruitment was resampled from 2002–2011, five catch scenarios were assumed, with future catch assumed to be the current catch (28% TACC reduction), 35% TACC reduction, 40% TACC reduction,

50% TACC reduction, or the current TACC (Figure C2, Tables C1–C5). When recruitment was resampled from 2010–2011, future catch was assumed to be the current catch (28% TACC reduction), 40% TACC reduction, or 50% TACC reduction (Figure C3, Tables C6–C8, Appendix C). It was further assumed that 85% of future commercial catch would be taken from the assessment area (the same as in 2015), and that the future recreational, customary, and illegal catch will be 15 t, 5 t, and 7.5 t respectively. The total catch used in the projections was 142 717 kg (28% reduction), 131 515 (35% reduction), 123 514 kg (40% reduction), 107 511 kg (50% reduction) and 187 524 kg (current TACC).

Projections were also carried out for MCMC 1.4, where future recruitment deviations were resampled from 2010–2011 and the future catch was assumed to be the current catch (28% TACC reduction), or 40% TACC reduction (Figure C4, Tables C9–C10, Appendix C).

The projections suggested that if future recruitment remains at long term average, the spawning stock abundance will increase to 22% (16–29%) of B_0 in 2018 at the current catch level (corresponding to a 28% TACC reduction), or 24% (18–31%) of B_0 with a 50% TACC reduction. If future recruitment is as low as that estimated in 2010 and 2011, the spawning stock abundance will increase slightly to 19% (14–25%) of B_0 in 2018 at the current catch level, or 21% (16–27%) of B_0 with a 50% TACC reduction. These projections suggest that the stock abundance is likely to increase over the next three years if future catch is the same or below the current level. However, it was extremely unlikely that the spawning stock biomass will be above the target (40% B_0) in the short term. If the catch remains the same and recruitment is below average, the probability of the spawning stock biomass in 2018 being below the soft limit (20% B_0) will be above 50%.

4. DISCUSSION

This report assesses the stock status for PAU 7 (Statistical Area 017 and 038 only). Estimates from the base case model suggest that the current spawning stock population ($B_{current}$) is 18% (16–21%) B_0, and recruit-sized stock abundance ($B^r_{current}$) is 9% (7–10%) of the initial state (B^r_r). The model suggested that the current stock status is likely to be below the soft limit. The projection suggested that biomass is likely to increase over the next three years if the future catch remains at or below the current catch level.

The model presented here, whilst fairly representing some of the data, also shows some indications of lack of fit. It is unlikely that the estimates of historical stock size are accurate, given assumptions about annual recruitment and the use of the historical catch-effort indices of abundance. The apparent decline of mean length in commercial catch in 2014 across the stock areas potentially indicated a decline in abundance. The model estimated an increase in abundance in 2014 and 2015, which was contrary to the trend in recent CPUE, although alternative indices developed using a more complex model that have taken into account spatial and temporal correlations of catch and effort indicated that the declining trend in PAU 7 might have been reversed over the last two years (Neubauer 2015).

CPUE provides information on changes in relative abundance. However, CPUE is generally considered to be a poor index of stock abundance for paua, due to divers' ability to maintain catch rates by moving from area to area despite a decreasing biomass (hyperstability). Breen & Kim (2003) argued that standardised CPUE might be able to relate to the changes of abundance in a fully exploited fishery such as PAU 7, and a large decline in the CPUE is most likely to reflect a decline in the fishery. Analysis of CPUE currently relies on paua Catch Effort Landing Return (PCELR) forms, which record daily fishing time and catch per diver on a relatively large spatial scale. These data are likely to remain the basis for stock assessments and formal management in the medium term. Since October 2010, a dive-logger data collection programme has been initiated to achieve fine-scale monitoring of paua fisheries

(Neubauer et al. 2015, Neubauer & Abraham 2014). The use of the data loggers by paua divers and ACE holders has been steadily increasing over the last three years. Using fishing data logged at fine spatial and temporal scales can substantially improve effort calculations and the resulting CPUE indices and allow complex metrics such as spatial CPUE to be developed (Neubauer & Abraham 2014). Data from the loggers have been analysed to provide comprehensive descriptions of the spatial extent of the fisheries and insight on relationships between diver behaviour, CPUE, and changes in abundance on various spatial and temporal scales (Neubauer et al. 2015, Neubauer & Abraham 2014, Neubauer 2015). However the data-loggers can potentially change how the divers operate such that they may become more effective in their fishing operations (the divers become capable of avoiding areas that have been heavily fished or that have relatively low CPUE without them having to go there to discover this), therefore changing the meaning of diver CPUE (Butterworth et al. 2015).

The current basis for the assumption of natural mortality is somewhat ad hoc, and the prior used is considered to be unduly informative (Butterworth et al. 2015). A revised prior has been investigated in this assessment. The prior was developed using a structured approach that assembles information from various QMAs for which reliable information on M is possible. The approach will only be feasible if the natural mortality of paua in other QMA is similar to PAU 7. If M varies significantly over large spatial scales (possibly due to temperature or other environmental factors), it would be inappropriate to use the information from other QMAs to inform natural mortality for PAU 7.

Heterogeneity in growth can be a problem for this kind of model (Punt 2003). Variation in growth is addressed to some extent by having a stochastic growth transition matrix based on increments observed in several different places; similarly the length frequency data are integrated across samples from many places. Relative weights have been assigned to the area in proportion to the catch so that more productive areas are better represented in the model. However, model results could be still be too optimistic. For instance, if some local stocks are fished very hard and others are not fished, recruitment failure can result because of the depletion of spawners. Spawners must breed close to each other and the dispersal of larvae is unknown and may be limited. Recruitment failure is a common observation in overseas abalone fisheries, suggesting that local processes may decrease recruitment, an effect that the current model cannot account for.

5. ACKNOWLEDGMENTS

This work was supported by a contract from the Ministry for Primary Industries (PAU201501 Objective 1). Thank you to Paul Breen for developing the stock assessment model that was used in this assessment and for the use of major proportions of the 2006 report for this update. Thank you to the Shellfish Working Group for all the advice provided throughout the assessment process. Thank you to Reyn Naylor for reviewing the draft report.

6. REFERENCES

Abraham, E.R. (2012). Paua catch per unit effort from logger data. Final Research Report for Ministry for Primary Industries project PAU2010-03 (Unpublished report held by Ministry for Primary Industries, Wellington).

Andrew, N.L.; Breen, P.A.; Naylor, J.R.; Kendrick, T.H.; Gerring, P. (2000). Stock assessment of paua (*Haliotis iris*) in PAU 7 in 1998–99. *New Zealand Fisheries Assessment Report 2000/49*. 40 p.

Breen, P.A.; Andrew, N.L.; Kendrick, T.H. (2000a). Stock assessment of paua (*Haliotis iris*) in PAU 5B and PAU 5D using a new length-based model. *New Zealand Fisheries Assessment Report 2000/33*. 37 p.

Breen, P.A.; Andrew, N.L.; Kendrick, T.H. (2000b). The 2000 stock assessment of paua (*Haliotis iris*) in PAU 5B using an improved Bayesian length-based model. *New Zealand Fisheries Assessment Report 2000/48*. 36 p.

Breen, P.A.; Andrew, N.L.; Kim, S.W. (2001). The 2001 stock assessment of paua (*Haliotis iris*) in PAU 7. *New Zealand Fisheries Assessment Report 2001/55*. 53 p.

Breen, P.A.; Kim, S.W. (2003). The 2003 stock assessment of paua (*Haliotis iris*) in PAU 7. *New Zealand Fisheries Assessment Report 2003/35.* 112 p.

Breen, P.A.; Kim, S.W. (2004a). The 2004 stock assessment of paua (*Haliotis iris*) in PAU 4. *New Zealand Fisheries Assessment Report 2004/55.* 79 p.

Breen, P.A.; Kim, S.W. (2004b). The 2004 stock assessment of paua (*Haliotis iris*) in PAU 5A. *New Zealand Fisheries Assessment Report 2004/40*. 86 p.

Breen, P.A.; Kim, S.W. (2005). The 2005 stock assessment of paua (*Haliotis iris*) in PAU 7. *New Zealand Fisheries Assessment Report 2005/47*. 114 p.

Breen, P.A.; Kim, S.W. (2007). The 2006 stock assessment of paua (*Haliotis iris*) stocks PAU 5A (Fiordland) and PAU 5D (Otago). *New Zealand Fisheries Assessment Report 2007/09*. 164 p.

Breen, P.A.; Kim, S.W.; Andrew, N.L. (2003). A length-based Bayesian stock assessment model for abalone. *Marine and Freshwater Research 54(5):* 619–634.

Breen, P.A.; Smith, A.N.H. (2008a). The 2007 assessment for paua *(Haliotis iris)* stock PAU 5B (Stewart Island). *New Zealand Fisheries Assessment Report 2008/05.*

Breen, P.A.; Smith, A.N.H. (2008b). Data used in the 2007 assessment for paua (*Haliotis iris*) stock PAU 5B (Stewart Island). *New Zealand Fishery Assessment Report 2008/6*. 45 p.

Bull, B.; Francis, R.I.C.C.; Dunn, A.; McKenzie, A.; Gilbert, D.J.; Smith, M.H.; Bian, R. (2012). CASAL (C++ algorithmic stock assessment laboratory): CASAL User Manual v2.30-2012/03/21. *NIWA Technical Report 135*.

Butterworth, D.; Haddon, M.; Haist, V.; Helidoniotis, F. (2015). Report on the New Zealand Paua stock assessment model; 2015. *New Zealand Fisheries Science Review 2015/4*. 10 p.

Cordue, P.L. (2009). Analysis of PAU5A dive survey data and PCELR catch and effort data. Final report for SeaFIC and PauaMAC5. (Unpublished report held by SeaFIC.)

Francis, R.I.C.C. (2011). Data weighting in statistical fisheries stock assessment models. *Canadian Journal of Fisheries and Aquatic Sciences* 68: 15.

Fu, D. (2012). The 2011 stock assessment of paua (*Haliotis iris*) for PAU 7. *New Zealand Fisheries Assessment Report 2012/27*. 56 p.

Fu, D. (2013). The 2012 stock assessment of paua (*Haliotis iris*) for PAU 5D. *New Zealand Fisheries Assessment Report 2013/57*. 56 p.

Fu, D. (2014a). The 2013 stock assessment of paua (*Haliotis iris*) for PAU 5B. *New Zealand Fisheries Assessment Report* 2014/45.

Fu, D. (2014b). The 2013 stock assessment of paua (*Haliotis iris*) for PAU 3. *New Zealand Fisheries Assessment Report* 2014/44. 51 p.

Fu, D. (2015a). The 2014 stock assessment of paua (*Haliotis iris*) for Chalky and South Coast in PAU 5A. *New Zealand Fisheries Assessment Report 2015/64.*

Fu, D. (2015b). The 2014 stock assessment of paua (*Haliotis iris*) for Milford, George, Central, and Dusky in PAU 5A. *New Zealand Fisheries Assessment Report 2015/65.*

Fu, D.; McKenzie, A. (2010a). The 2010 stock assessment of paua (*Haliotis iris*) for Chalky and South Coast in PAU 5A. *New Zealand Fisheries Assessment Report 2010/36.* 63 p.

Fu, D.; McKenzie, A. (2010b). The 2010 stock assessment of paua (*Haliotis iris*) for Milford, George, Central, and Dusky in PAU 5A. *New Zealand Fisheries Assessment Report 2010/46*. 55 p.

Fu, D.; McKenzie. A; Naylor, R. (2010). Summary of input data for the 2010 PAU 5A stock assessment. *New Zealand Fisheries Assessment Report 2010/35*. 58 p.

Fu, D.; McKenzie, A.; Naylor, J.R. (2012). Summary of input data for the 2011 PAU 7 stock assessment. *New Zealand Fisheries Assessment Report* 2012/26. 46 p.

Fu, D.; McKenzie, A; Naylor, R. (2013). Summary of input data for the 2012 PAU 5D stock assessment. *New Zealand Fisheries Assessment Report* 2013/56. 47 p.

Fu, D.; McKenzie, A; Naylor, R. (2014a). Summary of input data for the 2013 PAU 5B stock assessment. *New Zealand Fisheries Assessment Report* 2014/43. 61 p.

Fu, D.; McKenzie, A; Naylor, R. (2014b). Summary of input data for the 2013 PAU 3 stock assessment. *New Zealand Fisheries Assessment Report* 2014/42. 45 p.

Fu, D.; McKenzie, A; Naylor, R. (2015). Summary of input data for the 2014 PAU 5A stock assessment. *New Zealand Fisheries Assessment Report 2015/*68.

Fu, D.; McKenzie, A; Naylor, R. (submitted). Summary of input data for the 2015 PAU 7 stock assessment. New Zealand Fisheries Assessment Report.

Haist, V. (2010). Paua research diver survey: review of data collected and simulation study of survey method. *New Zealand Fisheries Assessment Report 2010/38*. 54 p.

Kim, S.W.; Bentley, N.; Starr, P.J.; Breen, P.A. (2004). Assessment of red rock lobsters (*Jasus edwardsii*) in CRA 4 and CRA 5 in 2003. *New Zealand Fisheries Assessment Report 2004/8*. 165 p.

McAllister, M.K.; Ianelli, J.N. (1997). Bayesian stock assessment using catch-age data and the sampling - importance resampling algorithm. *Canadian Journal of Fisheries and Aquatic Sciences* 54(2): 284–300.

McKenzie, A.; Smith, A.N.H. (2009a). The 2008 stock assessment of paua (*Haliotis iris*) in PAU 7. *New Zealand Fisheries Assessment Report 2009/34.* 84 p.

McKenzie, A.; Smith, A.N.H. (2009b). Data inputs for the PAU 7 stock assessment in 2008. *New Zealand Fisheries Assessment Report 2009/33.* 34 p.

McShane, P.E.; Mercer, S.F.; Naylor, J.R. (1994). Spatial variation and commercial fishing of the New Zealand paua (*Haliotis iris* and *H. australis*). *New Zealand Journal of Marine and Freshwater Research* 28: 345–355.

McShane, P.E.; Mercer, S.; Naylor, J.R.; Notman, P.R. (1996). Paua (*Haliotis iris*) fishery assessment in PAU 5, 6, and 7. New Zealand Fisheries Assessment Research Document 96/11. 35 p. (Unpublished report held in NIWA library, Wellington.)

Murray, T.; Akroyd, J. (1984). The New Zealand paua fishery: an update and review of biological considerations to be reconciled with management goals. Fisheries Research Centre Internal Report 5. 25 p. (Unpublished report held in NIWA library Wellington.)

Neubauer, P. (2015). Alternative CPUE indices for PAU7, 11 pages. (Unpublished report held by Ministry for Primary Industries.)

Neubauer, P.; Abraham, E. (2014). Using GPS logger data to monitor change in the PAU 7 pāua (*Haliotis iris*) fishery. *New Zealand Fisheries Assessment Report. 2014/31* 18.

Neubauer, P.; Abraham, E.; Know, C.; Richard, Y. (2015). Assessing the performance of paua (*Haliotis iris*) fisheries using GPS logger data. *New Zealand Fisheries Assessment Report 2015/71*.

Punt, A.E. (2003). The performance of a size-structured stock assessment method in the face of spatial heterogeneity in growth. *Fisheries Research 65:* 391–409.

Schiel, D.R. (1989). Paua fishery assessment 1989. New Zealand Fisheries Assessment Research Document 89/9: 20 p. (Unpublished report held in NIWA library, Wellington, New Zealand.)

Schiel, D.R. (1992). The paua (abalone) fishery of New Zealand. *In:* Abalone of the world: Biology, fisheries and culture. Shepherd, S.A.; Tegner, M.J.; Guzman del Proo, S. (eds.) pp. 427–437. Blackwell Scientific, Oxford.

Schiel, D.R.; Breen, P.A. (1991). Population structure, ageing and fishing mortality of the New Zealand abalone *Haliotis iris*. *Fishery Bulletin 89*: 681–691.

Schnute, J. (1985). A General Theory for Analysis of Catch and Effort Data. *Canadian Journal of Fisheries and Aquatic Sciences 42(3)*: 414–429.

Shepherd, S.A.; Breen, P.A. (1992). Mortality in abalone: its estimation, variability and causes. *In*: 'Abalone of the World: Biology, Fisheries and Culture'. (Eds S.A. Shepherd, M.J. Tegner, and S. Guzman del Proo.) pp. 276–304. (Blackwell Scientific: Oxford.)

Shepherd, S.A.; Rodda, K.R.; Vargas, K.M. (2001). A chronicle of collapse in two abalone stocks with proposals for precautionary management. *Journal of Shellfish Research 20:* 843–856.

Table 1: Actual sample sizes, initial sample sizes determined for the multinomial likelihood, and model weighted sample sizes for the PAU 7 commercial catch sampling length frequencies from the base case (1.0) and the initial model run (0.9). The base case used the Francis (1991) method and model 0.9 used the McAllister & Ianelli (1997) method. A description of the initial runs are summarised in A1. A description of the base case is given in Table 4.

Fishing year	Actual sample size	Initial sample size	1.0	0.9
1990	4 726	897	37	215
1991	9 577	1 240	51	215
1992	8 759	1 437	59	215
1993	7 027	1 328	54	215
1994	8 752	2 118	87	215
1999	5 199	1 604	66	215
2000	5 170	1 402	57	215
2001	3 466	958	39	215
2002	6 271	2 508	103	215
2003	6 421	2 069	85	215
2004	4 174	1 589	65	215
2005	4 022	1 202	49	215
2006	2 641	1 000	41	215
2007	5 463	1 485	61	215
2008	9 354	1 536	63	215
2009	5 389	1 220	50	215
2010	10 789	3 212	132	215
2011	16 327	4 625	190	215
2012	22 514	5 798	238	215
2013	22 172	4 682	192	215
2014	18 219	5 456	224	215
2015	19 622	4 519	185	215

Table 2: Base case model specifications: for estimated parameters, the phase of estimation, type of prior, (U, uniform; N, normal; LN, lognormal), mean and CV of the prior, lower bound and upper bound.

Parameter	Phase	Prior	μ	CV	Lower	Upper
ln($R0$)	1	U	–	–	5	50
M	3	LN	0.1	0.1	0.01	0.5
g_{max}	2	U	–	–	1	50
$g_{50\%}$	2	U	–	–	0.01	150
$g_{50\text{-}95\%}$	2	U			0.01	150
φ	2	U	–	–	0.001	1
$Ln(q^I)$	1	U	–	–	-30	0
$Ln(q^J)$	1	U	–	–	-30	0
$Ln(q^k)$	1	U	–	–	-30	0
L_{50}	1	U	–	–	70	145
$L_{95\text{-}50}$	1	U	–	–	1	50
T_{50}	2	U	–	–	70	125
$T_{95\text{-}50}$	2	U	–	–	0.001	50
D_{50}	2	U	–	–	70	145
$D_{95\text{-}50}$	2	U	–	–	0.01	50
ε	1	N	0	0.4	-2.3	2.3
D_s	1	U	–	–	0.01	10

Table 3: Values for fixed quantities for base case model.

Variable	Value
L_1	75
L_2	120
a	2.99E-08
b	3.303
U^{max}	0/80
σ_{min}	1
σ_{obs}	0.25
$\tilde{\sigma}$	0.2
H	0.75

Table 4: Summary descriptions of base case and sensitivity model runs.

Model	Description
1.0	base case, Francis (2011) weighting, inverse logistic, excluded Staircase growth, growth data weighted
1.1	1.0, CV for CPUE2 = 0.5
1.2	1.0, CV for CPUE2 = 1.2
1.3	1.0, estimated CPUE shape parameter with a uniform prior [0.5,1.5]
1.3a	1.0, CPUE shape parameter = 0.5
1.3b	1.0, CPUE shape parameter = 1.5
1.4	1.0, M estimated with a prior developed using information from PAU 5A and PAU 5B.
1.5	1.0, included Staircase growth

Table 5: MPD estimates for base case and sensitivity trials. "–" indicates parameter fixed and likelihood contributions not used when datasets were removed. SDNRs for CSLF were calculated from mean length. "Weights" means CV for CPUE indices and mean sample size for length frequency data.

Model runs	1.0	1.1	1.2	1.3	1.3a	1.3b	1.4	1.5
Likelihoods								
CPUE	-14.5	-14.7	-14.5	-14.4	-14.2	-14.5	-14.8	-14.4
PCPUE	-19.2	-26.4	-13.1	-19.7	-12.4	-20.9	-18.7	-18.2
CSLF	48.1	41.8	55.7	47.5	40.2	37.4	48.8	41.2
FBLF	11.5	11.6	11.3	11.4	11.8	10.9	11.8	6.2
Tags	1000.8	1001.3	999.9	999.7	1006.3	995.7	999.4	1166.9
Maturity	-51.7	-51.7	-51.7	-51.7	-51.7	-51.7	-51.7	-51.7
Prior on M	-0.2	-0.3	0.0	-0.1	-1.0	0.8	-0.4	0.5
Prior on ε	4.3	4.7	4.1	4.4	4.3	4.8	3.4	3.9
U penalty	0.1	0.1	0.0	0.1	0.1	0.0	0.1	0.0
ε penalty	0.0	0.0	0.0	0.0	0.0	0.0	0.0	0.0
Total	979.1	966.2	991.7	977.2	983.4	962.6	977.9	1134.5
Parameters								
ln(R0)	14.3	14.3	14.3	14.3	14.3	14.4	14.4	14.5
M	0.12	0.12	0.12	0.12	0.11	0.12	0.14	0.12
T_{50}	92.0	92.0	92.0	92.0	92.0	92.0	92.0	92.0
$T_{95\text{-}50}$	8.6	8.6	8.6	8.6	8.6	8.6	8.6	8.6
D_{50}	123.7	123.7	123.75	123.71	123.7	123.6	123.7	123.7
$D_{95\text{-}50}$	2.5	2.5	2.55	2.53	2.5	2.5	2.5	2.5
D_{shift}	0.9	0.9	0.85	0.87	0.8	0.9	0.9	0.8
L_{50}	140.9	141.6	139.8	140.3	143.5	137.7	141.6	135.7
$L_{95\text{-}50}$	13.8	14.3	13.2	13.6	14.4	11.9	14.1	9.4
$\ln(q^{I})$	-12.8	-12.8	-12.8	-14.2	-6.5	-18.9	-12.8	-12.8
$\ln(q^{I2})$	-12.2	-12.3	-12.2	-13.6	-6.2	-18.2	-12.2	-12.3
h	1.00	1.00	1.00	1.11	0.50	1.50	1.00	1.00
g_{α}	–	–	–	–	–	–	–	–
g_{β}	–	–	–	–	–	–	–	–
g_{max}	103.1	104.0	101.8	102.5	106.0	99.9	101.5	99.7
$g_{50\%}$	32.9	31.8	34.8	34.2	27.5	38.9	35.7	49.1
$g_{50\text{-}95\%}$	30.9	30.0	32.3	31.6	27.7	34.4	32.7	23.3
α	3.3	3.4	3.3	3.2	3.6	2.7	3.3	1.2
β	0.1	0.1	0.1	0.1	0.1	0.2	0.1	0.6
Indicators								
B0	4275	4272	4273	4261	4400	4218	3773	4392
Bcurrent	739	736	734	722	878	675	779	877
Bcurrent/B0	0.17	0.17	0.17	0.17	0.20	0.16	0.21	0.20
rB0	3564	3556	3575	3564	3612	3569	3054	3550
rBcurrent	286	287	282	278	363	262	291	290
rBcurrent/rB0	0.08	0.08	0.08	0.08	0.10	0.07	0.10	0.08
Ucurrent	0.48	0.48	0.49	0.50	0.38	0.53	0.49	0.47

Table 5–continued

Weights								
CPUE	0.10	0.10	0.10	0.10	0.10	0.10	0.10	0.10
PCPUE	0.08	0.05	0.12	0.08	0.08	0.08	0.08	0.08
CSLF	96	79	116	93	82	65	96	80
FBLF	100	100	100	100	100	100	100	100
SDNRs								
CPUE	0.59	0.57	0.59	0.60	0.63	0.60	0.55	0.61
PCPUE	0.69	0.61	0.73	0.63	1.20	0.47	0.74	0.78
CSLF	0.99	1.00	1.00	1.01	1.00	1.00	0.94	1.00
FBLF	0.97	0.98	0.97	0.97	0.99	0.95	0.99	0.71
Tags	0.99	0.99	0.98	0.98	1.01	0.97	0.98	1.03
Maturity	0.66	0.66	0.66	0.66	0.66	0.66	0.66	0.66

Table 6: Summary of the median of marginal posterior distributions for estimated parameters and key indicators from the MCMC chain from the base case and sensitivities. The numbers in the bracket show the 5th and 95th percentiles. Biomass is in tonnes.

	MCMC 1.0	MCMC 1.1	MCMC 1.2	MCMC 1.3	MCMC 1.4	MCMC 1.5
Parameters						
f	1004 (997–1013)	991 (984–1000)	1017 (1009–1026)	1004 (996–1013)	1003 (996–1012.)	1159 (1152–1168)
ln(*R0*)	14.3 (14.3–14.4)	14.3 (14.3–14.4)	14.4 (14.3–14.4)	14.3 (14.3–14.4)	14.4 (14.3–14.6)	14.5 (14.4–14.6)
M	0.11 (0.1–0.13)	0.11 (0.1–0.13)	0.11 (0.1–0.13)	0.11 (0.1–0.13)	0.14 (0.11–0.18)	0.12 (0.11–0.13)
T_{50}	142 (138.7–144.6)	142.2 (138.9–144.6)	141.6 (138–144.5)	142.3 (139–144.7)	142.6 (139–144.7)	136.4 (134–139.8)
$T_{95\text{-}50}$	14 (10.7–17.6)	14.2 (11–17.7)	13.7 (10.5–17.4)	13.9 (10.8–17.4)	14 (11–17.4)	10.8 (6.8–17.1)
D_{50}	123.8 (123.5–124)	123.7 (123.5–124)	123.8 (123.6–124)	123.8 (123.5–124)	123.7 (123.5–124)	123.7 (123.5–124)
$D_{95\text{-}50}$	2.6 (2.2–3)	2.5 (2.1–3)	2.6 (2.2–3)	2.6 (2.1–3)	2.5 (2.1–3)	2.5 (2.1–3)
D_{shift}	0.8 (0.2–1.4)	0.8 (0.2–1.5)	0.8 (0.2–1.4)	0.8 (0.2–1.4)	0.9 (0.3–1.5)	0.8 (0.2–1.4)
L_{50}	92 (91.3–92.7)	92 (91.3–92.7)	92 (91.3–92.7)	92 (91.3–92.7)	92 (91.3–92.7)	92 (91.3–92.7)
$L_{95\text{-}50}$	8.7 (7.2–10.5)	8.7 (7.2–10.5)	8.8 (7.2–10.5)	8.8 (7.2–10.6)	8.8 (7.2–10.6)	8.8 (7.2–10.6)
$\ln(q^{I})$	12.9 (13–12.7)	12.9 (13–12.7)	12.9 (13–12.7)	10.9 (13.98.7)	12.8 (13–12.7)	12.9 (13–12.7)
$\ln(q^{I2})$	12.3 (12.4–12.2)	12.3 (12.4–12.2)	12.3 (12.4–12.1)	10.4 (13.38.2)	12.3 (12.4–12.2)	12.3 (12.4–12.2)
α	3.53 (2.82–4.11)	3.49 (2.84–4.05)	3.53 (2.78–4.12)	3.61 (2.9–4.13)	3.48 (2.65–4.17)	1.26 (0.96–1.63)
β	0.12 (0.05–0.21)	0.12 (0.06–0.21)	0.12 (0.05–0.21)	0.11 (0.05–0.2)	0.12 (0.05–0.23)	0.65 (0.54–0.76)
g_{max}	30 (26.3–36.1)	29.8 (26–35.1)	30.5 (26.4–37.2)	29.3 (25.8–35)	31.9 (27.2–39.9)	23.7 (19.9–29.2)
$g_{50\%}$	103.7 (98.5–107.1)	104 (99.3–107.3)	103.3 (97.6–107)	104.4 (99.5–107.6)	102 (95.4–106.3)	98.5 (91.5–104.2)
$g_{50\text{-}95\%}$	30.9 (25.9–37.4)	30.7 (25.9–36.5)	31.5 (26.1–38.4)	29.7 (24.7–36.3)	33.7 (27.5–41.8)	49.2 (43.9–55.1)
h	–	–	–	0.84 (0.66–1.08)	–	–

Table 6–continued.

	MCMC 1.0	MCMC 1.1	MCMC 1.2	MCMC 1.3	MCMC 1.4	MCMC 1.5
B_0	4291 (3980–4584)	4296 (3963–4600)	4296 (3968–4610)	4322 (4011–4632)	3784 (3185–4359)	4404 (4118–4687)
B_{msy}	1133 (1056–1209)	1133 (1051–1212)	1137 (1053–1216)	1137 (1060–1216)	1019 (913–1153)	1231 (1162–1299)
$B_{current}$	780 (689–888)	763 (689–855)	786 (683–919)	804 (701–938)	821 (723–937)	902 (783–1064)
$B_{current}$ $(\%B_0)$	0.18 (0.16–0.21)	0.18 (0.15–0.21)	0.18 (0.16–0.22)	0.19 (0.16–0.22)	0.22 (0.17–0.28)	0.21 (0.17–0.25)
$B_{current}$ $(\%B_{msy})$	0.69 (0.59–0.81)	0.68 (0.58–0.79)	0.69 (0.59–0.83)	0.71 (0.6–0.85)	0.81 (0.65–0.98)	0.74 (0.63–0.87)
B_{msy} $(\%B_0)$	0.26 (0.26–0.27)	0.26 (0.26–0.27)	0.26 (0.26-0.27)	0.26 (0.26–0.27)	0.27 (0.26–0.29)	0.28 (0.28–0.28)
rB_0	3532 (3185–3842)	3543 (3184–3876)	3538 (3179-3872)	3544 (3210–3876)	3019 (2395–3605)	3537 (3226–3839)
rB_{msy}	544 (438–638)	546 (443–648)	547 (439-649)	539 (442–643)	414 (279–571)	505 (410–598)
rBcurrent	300 (260–349)	297 (265–336)	302 (251-364)	314 (265–382)	306 (266–351)	300 (259–349)
$rB_{current}$ (rB_0)	0.09 (0.07–0.1)	0.08 (0.07–0.1)	0.09 (0.07-0.11)	0.09 (0.07–0.11)	0.1 (0.08–0.13)	0.09 (0.07–0.1)
$rB_{current}$ (rB_{msy})	0.55 (0.43–0.74)	0.55 (0.43–0.71)	0.55 (0.42-0.76)	0.59 (0.44–0.79)	0.74 (0.51–1.15)	0.59 (0.47–0.78)
rB_{msy} $(\%rB_0)$	0.15 (0.14–0.17)	0.15 (0.14–0.17)	0.15 (0.14-0.17)	0.15 (0.14–0.17)	0.14 (0.11–0.16)	0.14 (0.13–0.16)
MSY	207 (202–214)	207 (201–213)	208 (202-215)	207 (201–214)	217 (206–234)	205 (199–213)
U_{msy}	0.37 (0.31–0.47)	0.37 (0.3–0.46)	0.37 (0.31-0.47)	0.37 (0.31–0.47)	0.51 (0.35–0.79)	0.39 (0.33–0.5)
$U_{\%40B0}$	0.19 (0.16–0.23)	0.18 (0.16–0.22)	0.19 (0.16-0.23)	0.19 (0.16–0.22)	0.25 (0.18–0.4)	0.2 (0.17–0.25)
$U_{current}$	0.46 (0.4–0.52)	0.46 (0.41–0.5)	0.46 (0.38-0.54)	0.44 (0.36–0.51)	0.46 (0.41–0.52)	0.46 (0.4–0.51)

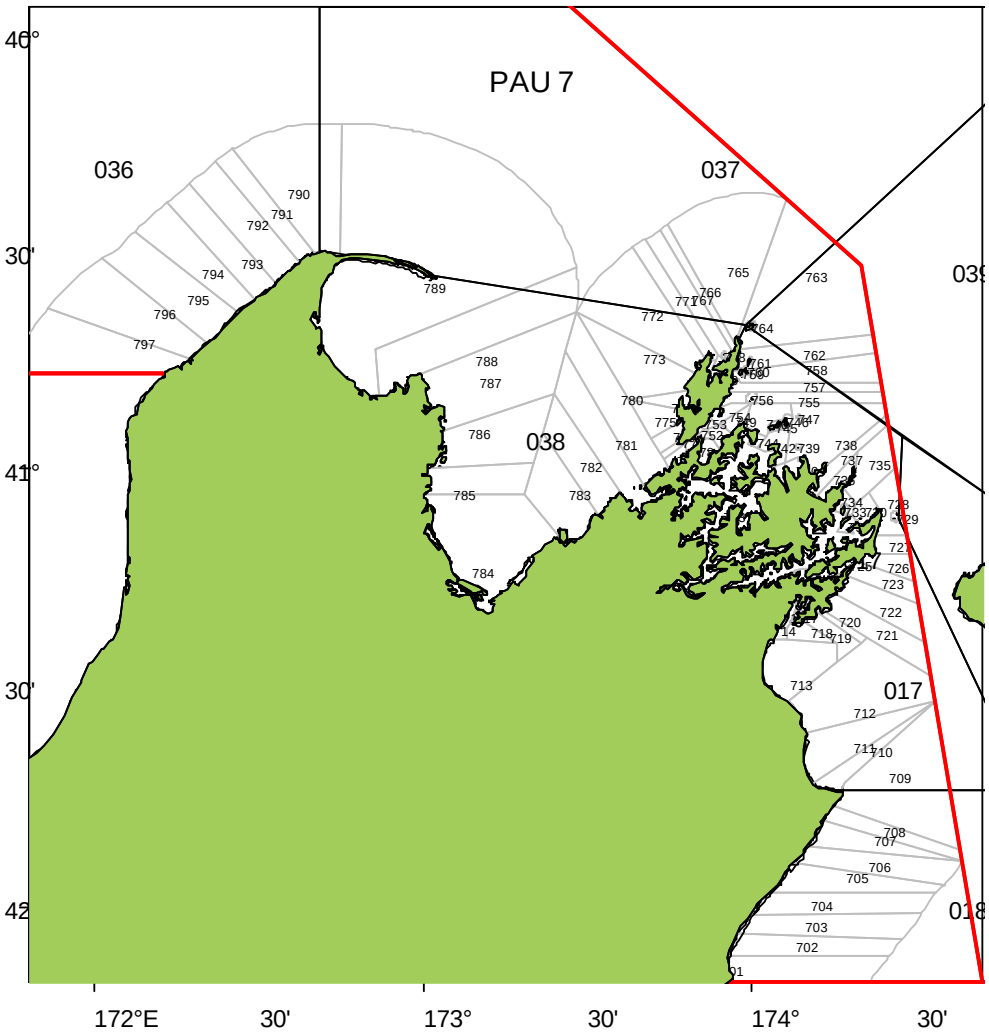

Figure 1: Map of PAU 7 showing the boundaries of the general statistical areas and the new finer scale Paua statistical areas.

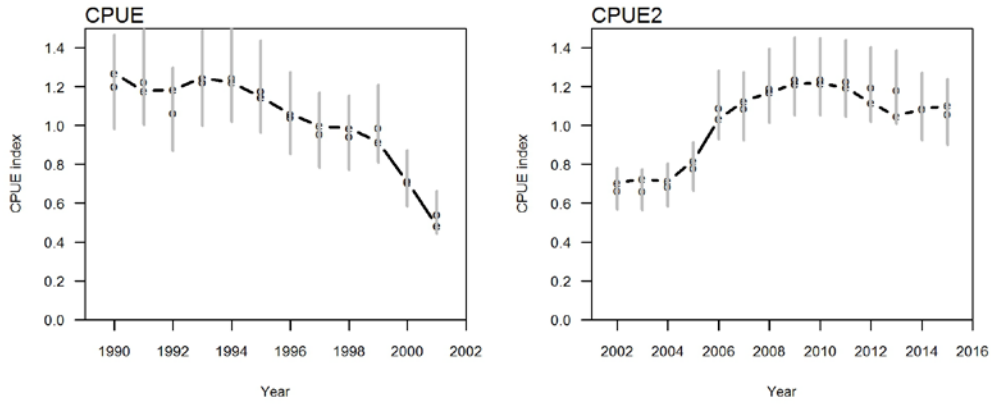

Figure 2: Fits to the CPUE indices 1990–2001 (left) and 2002–2015 indices (right), for MPD 1.0 (base case).

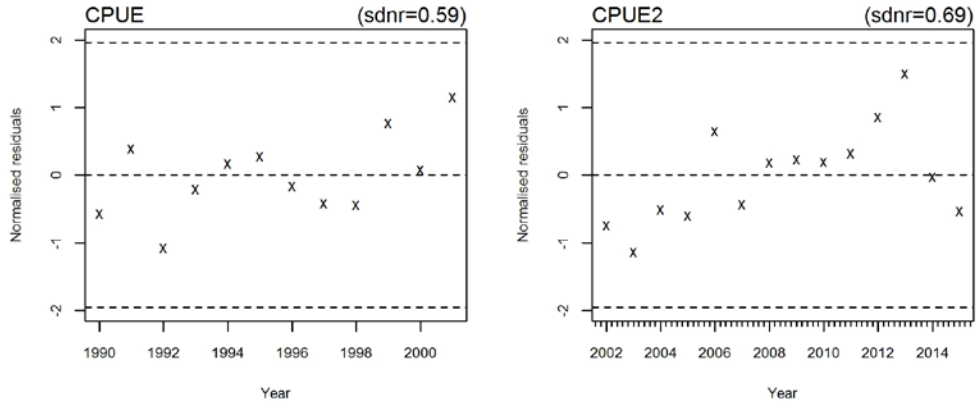

Figure 3: Normalised residuals from fits to the two CPUE datasets for MPD 1.0 (base case).

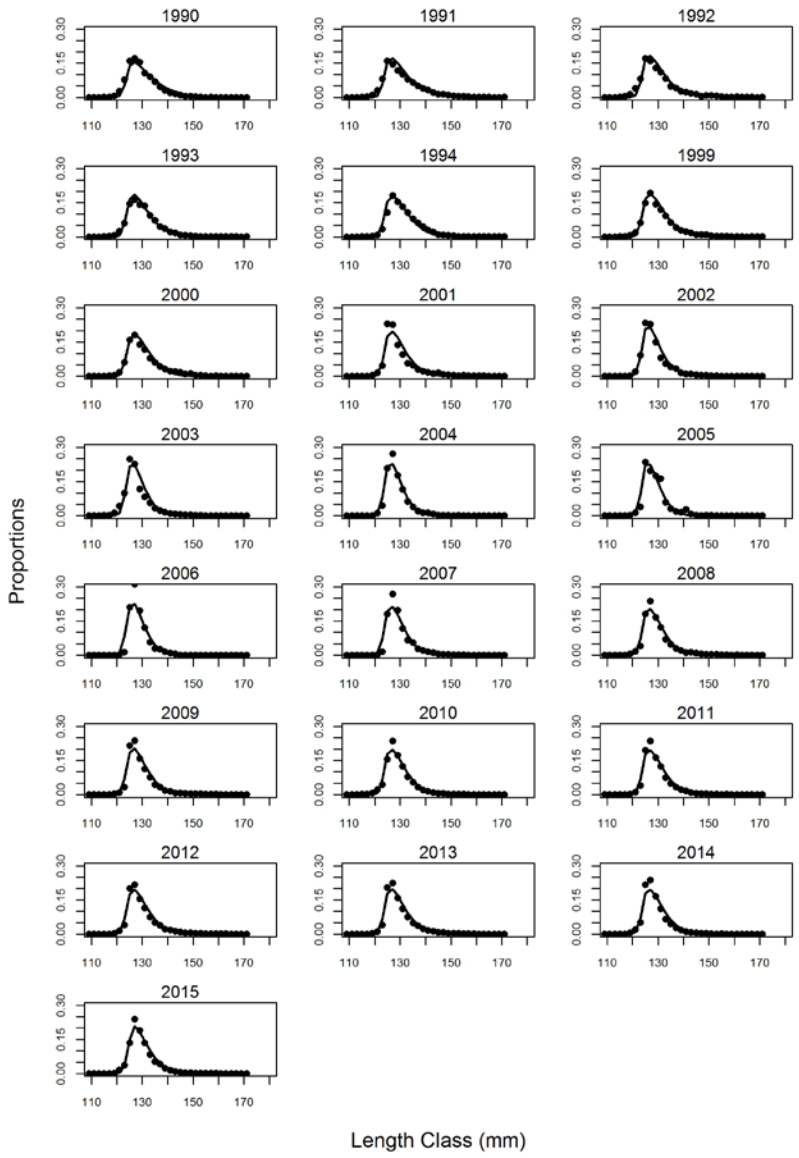

Figure 4: Fits to the CSLF data 1990–1994, 1999–2015 for MPD 1.0 (base case).

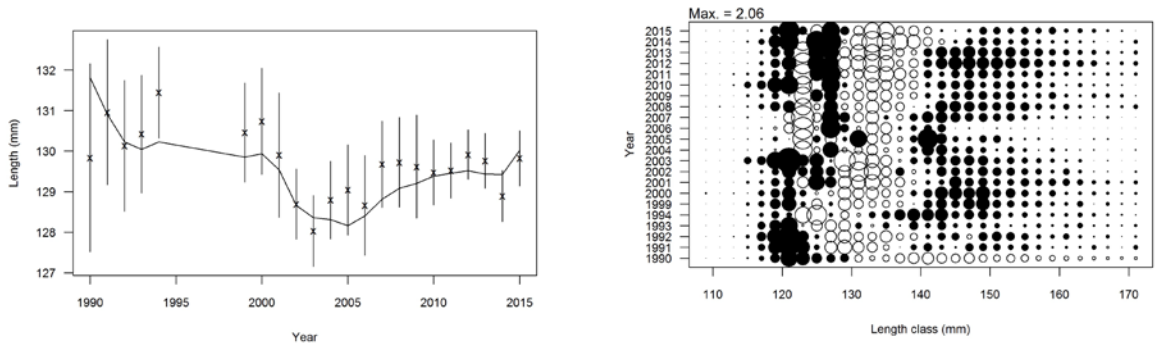

Figure 5: observed and predicted mean length by year for the CSLF (left) and normalised residuals from fits MPD 1.0 (base case). The size of the circle is proportional to the value. Black circles represent negative residuals and white circles represent positive residuals.

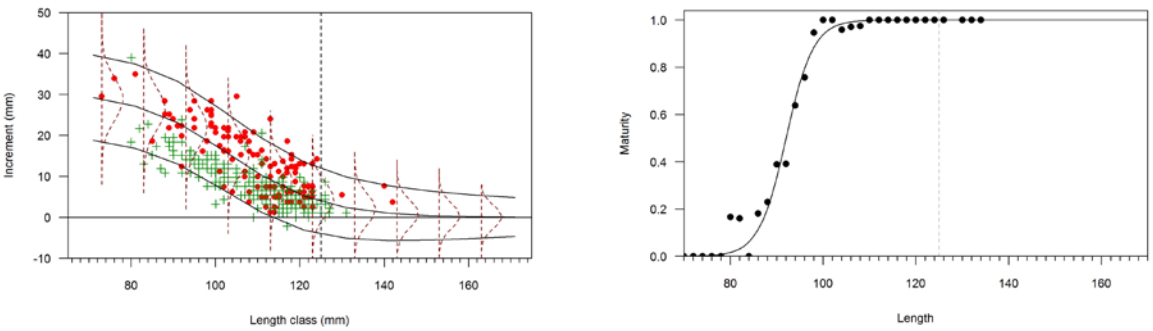

Figure 6: **Fits to the tag-recapture data (left) and fits to the length-at-maturity data for MPD 1.0 (base case). For the fits to the tag-recapture data, dots are observed mean annual increments; the lines are the fitted growth curve with 95% confidence intervals at selected sizes**.

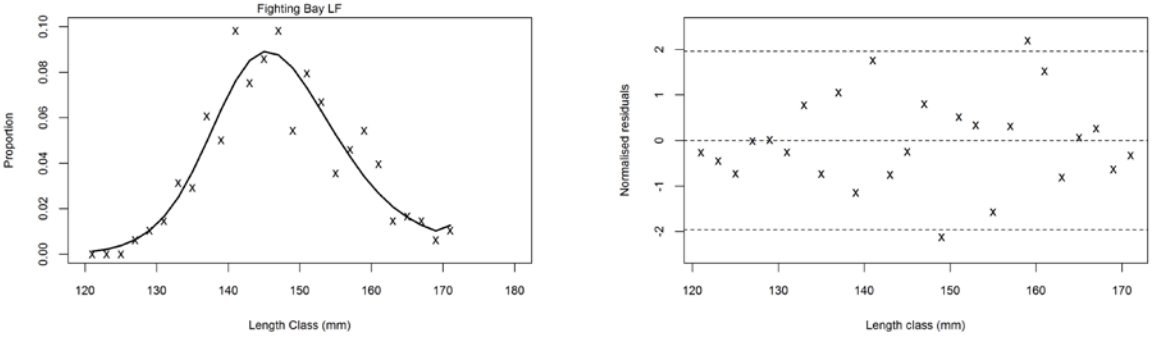

Figure 7: Fits to the FBLF data (left) and Normalised residuals by length class (right) for MPD 1.0.

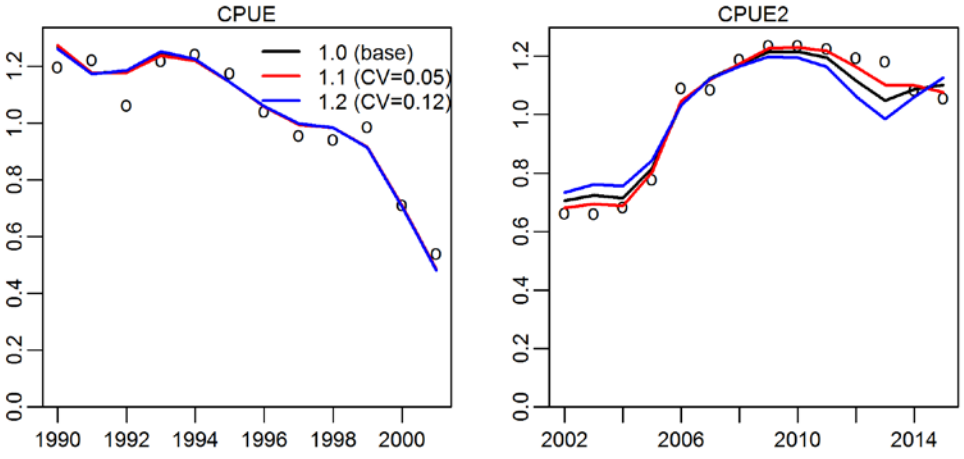

Figure 8: Comparison of Fits to the CPUE 1990–2001 (left) and 2002–2015 (right), for MPD 1.0, 1.1, 1.2.

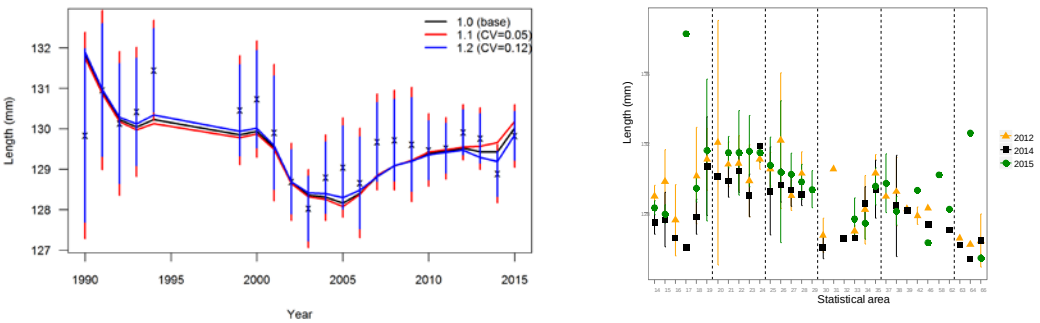

Figure 9: Comparison of predicted mean length by year to for the CSLF for MPD 1.0, 1.1, and 1.2 (left), and observed mean length by statistical area from commercial catch sampling (right) for 2011, 2014, and 2015 (right).

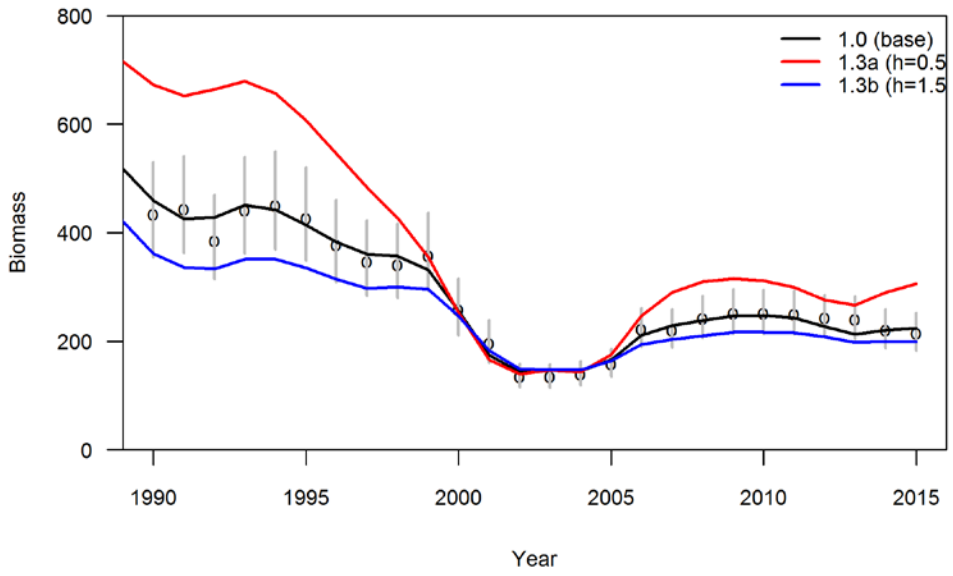

Figure 10: Comparison of predicted vulnerable (to fishing) biomass for MPD 1.0, 1.3a, and 1.3b, overlaid with observed CPUE indices (scaled by estimated catchability).

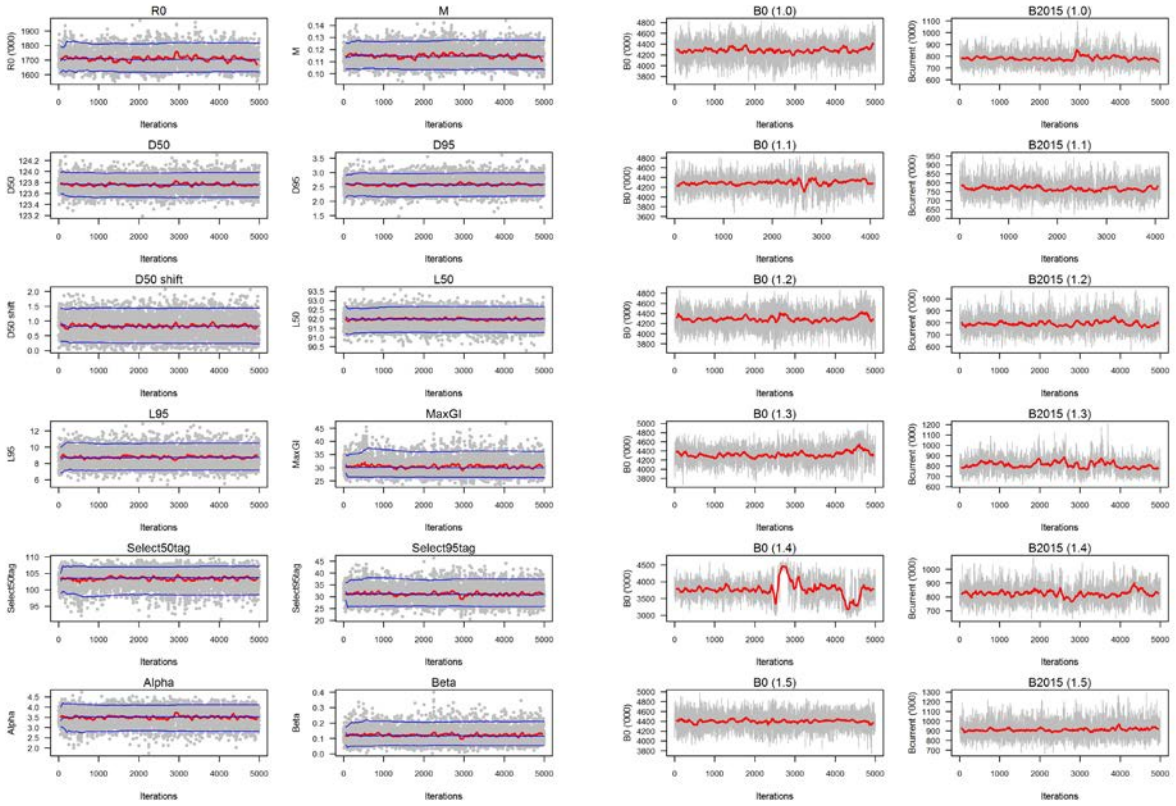

Figure 11: Traces of posterior samples for estimated parameters for MCMC 1.0 (base case) (left), and for biomass indicators for MCMC 1.0, 1.1, 1.2, 1.3, 1.4, and 1.5 (right). Blues lines are running 5, 50, and 95% quantiles of the chain and red lines are the moving average of the chain.

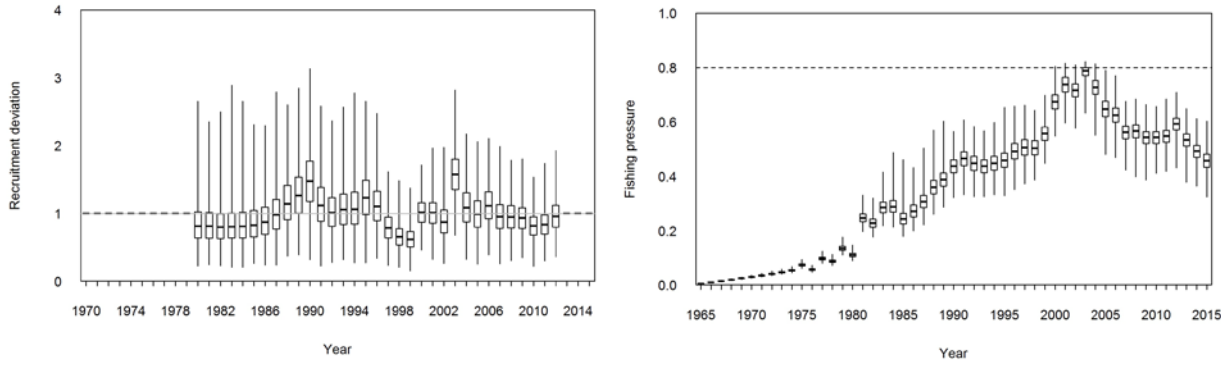

Figure 12: Posterior distributions of recruitment deviations (left), and exploitation rates (right) for MCMC 1.0. The box shows the median of the posterior distribution (horizontal bar), the 25th and 75th percentiles (box), with the whiskers representing the full range of the distribution. Recruitment deviations were estimated for 1980–2012, and fixed at 1 for other years. Maximum exploitation rate was assumed to be 0.8.

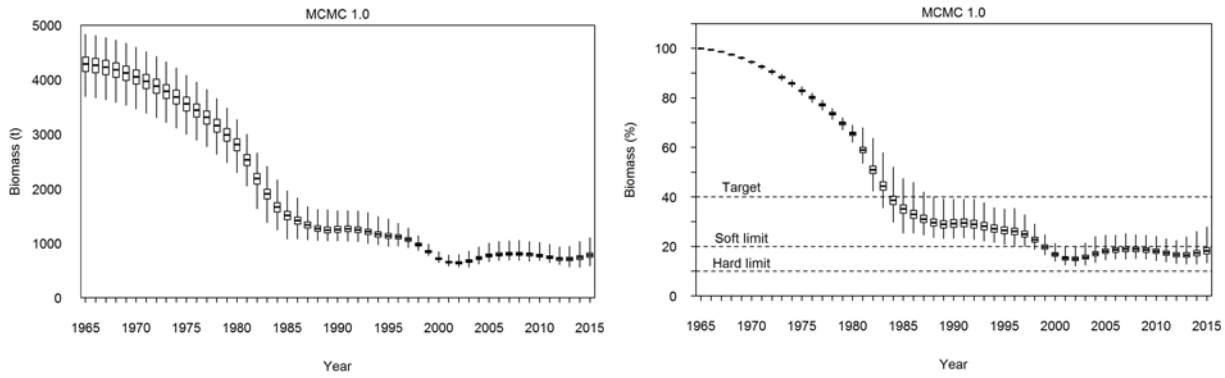

Figure 13: Posterior distributions of spawning stock biomass and spawning stock biomass as a percentage of virgin level from MCMC 1.0. The box shows the median of the posterior distribution (horizontal bar), the 25th and 75th percentiles (box), with the whiskers representing the full range of the distribution.

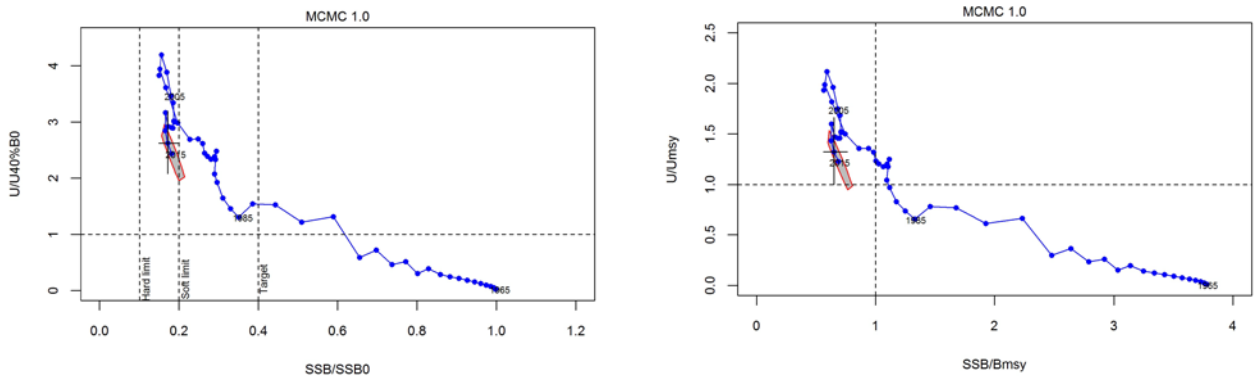

Figure 14: Trajectory of exploitation rate as a ratio of $U_{\%40B0}$ and spawning stock biomass as a ratio of B_0 (left), and exploitation rate as a ratio of U_{msy} and spawning stock biomass as a ratio of B_{msy} from the start of assessment period 1965 to 2015 for MCMC 1.0 (base case). The vertical lines at 10%, 20% and 40% B_0 represent the soft limit, the hard limit, and the target. Estimates are based on MCMC median and the 2015 90% marginal CI is shown by the cross line, and joint CI is shown by the grey area.

MCMC 1.0 MCMC 1.1 MCMC 1.2

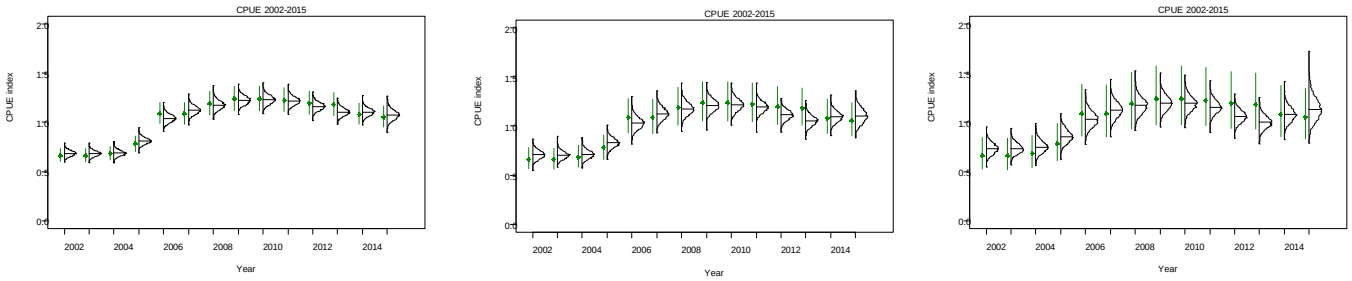

Figure 15 : Posterior distributions of model predicted CPUE indices for 2002–2015 for MCMC 1.0, 1.1 and 1.2 (Medians are shown as horizontal lines). Dots are observed CPUE indices and vertical lines are 95% confidence intervals.

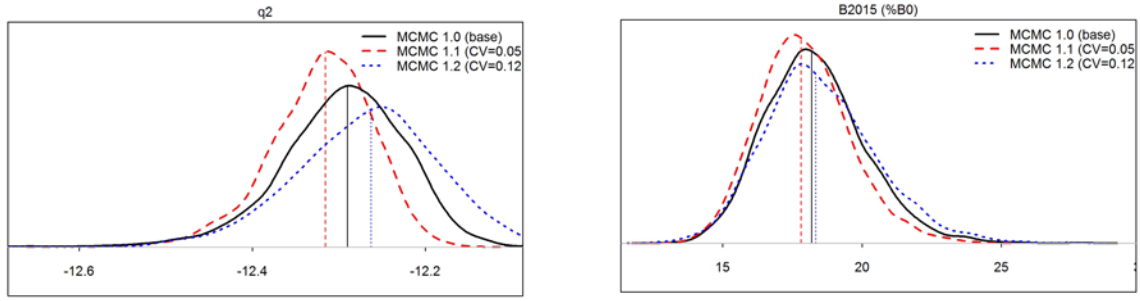

Figure 16: Posterior density of estimated catchability q of CPUE series 2002–2015 (left), and of estimated stock status $B_{current}$ as a percent of B_0 for MCMC 1.0 (base case), 1.1, and 1.2 (right). The vertical lines indicate the median of the corresponding posterior distribution.

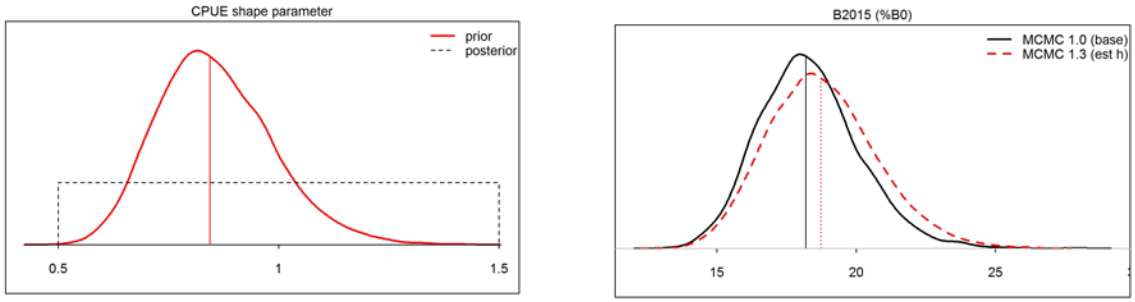

Figure 17: Posterior density of estimated CPUE shape parameter for MCMC 1.3 (left), and of estimated stock status $B_{current}$ as a percent of B_0 for MCMC 1.0 (base case) and 1.3 (right). The vertical lines indicate the median of the corresponding posterior distribution.

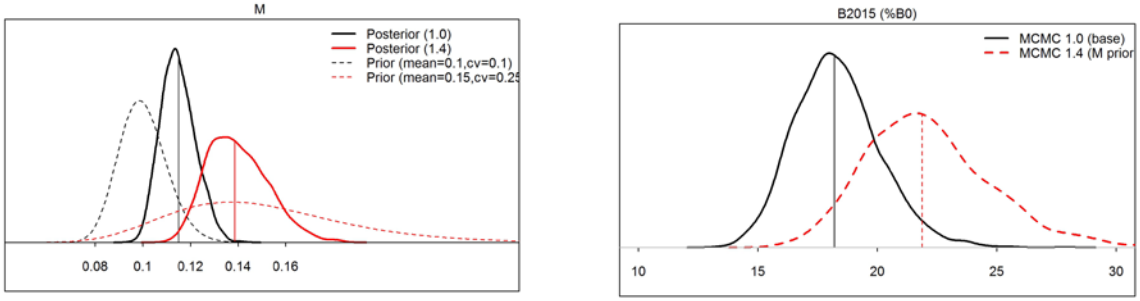

Figure 18: Prior and posterior density of *M* (left), and of estimated stock status $B_{current}$ as a percent of B_0 for MCMC 1.0 (base case) and 1.4 (right). The vertical lines indicate the median of the corresponding posterior distribution.

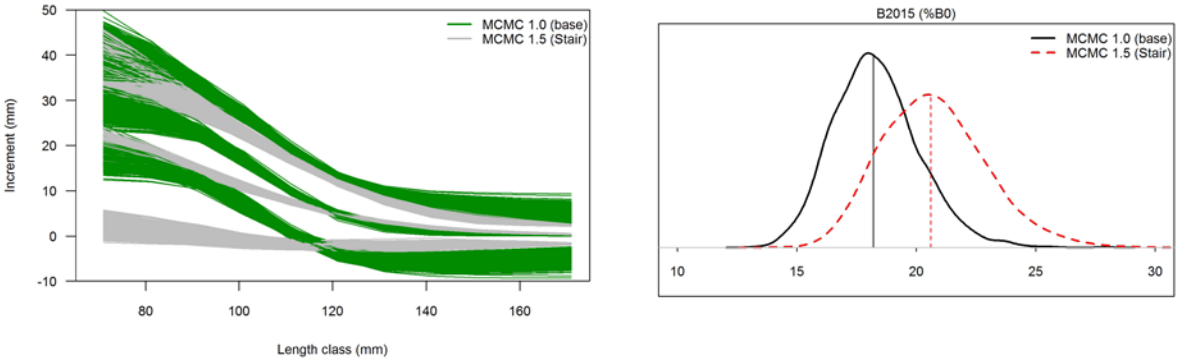

Figure 19: Estimated mean growth rates with 95 confidence interval from all posterior samples for MCMC 1.5 (left), and posterior density of estimated stock status $B_{current}$ as a percent of B_0 for MCMC 1.0 (base case) and 1.5 (right). The vertical lines indicate the median of the corresponding posterior distribution.

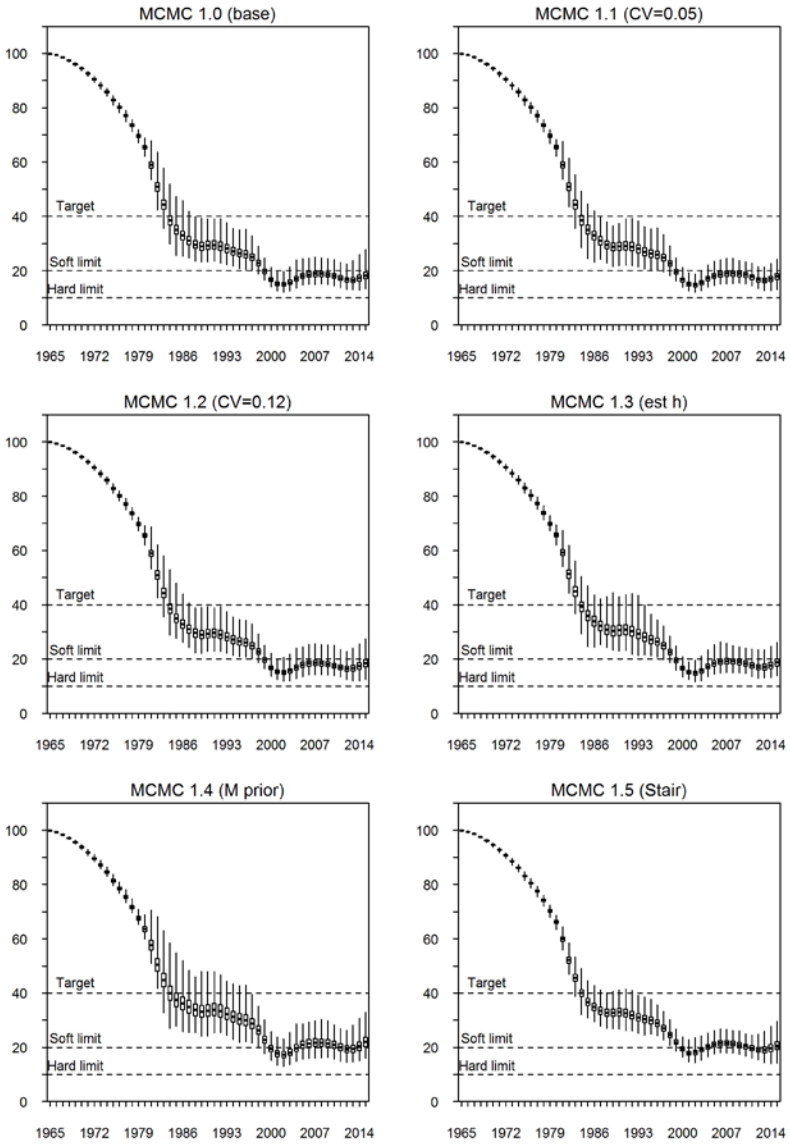

Figure 20: Posterior distributions spawning stock biomass as a percentage of virgin level from MCMC 1.0, 1.1, 1.2, 1.3, 1.4, and 1.5. The box shows the median of the posterior distribution (horizontal bar), the 25th and 75th percentiles (box), with the whiskers representing the full range of the distribution.

APPENDIX A: SUMMARY OF RESULTS FOR MPD INITIAL MODEL RUNS

Table A.1: Summary descriptions of Initial MPD model runs. "Half M" , if CPUE was calculated after half of natural mortality occurred; "CPUE" and "CPUE2", the assumed CV for CPUE indices; "CSLF", weighting method being used: "F" for Francis (2011) weighting method and "M" for McAllister & Ianelli (1997) method; "Model", growth model being used: "Exp" for exponential model" and "Inv" for inverse-logistic model; "Staircase", whether growth increment data from the Staircase are included; "Negative", if the growth transition matrix permits negative growth; "Weight", if the growth data are weighted by the area catch. Run i_0.4ext and i_0.5ext covered size classes 2–170mm. Run i_0.7b included FBLF data. Run i_0.11, the commercial catch for 1981–1983 was based on Murray & Akroyd (1984) instead of Schiel (1992). Run i_0.12 used alterative CPUE indices 2002–2015 as developed by Neubauer (2015). Run i_0.12 used a combined indices covering 1990–2015 (se Fu et al. 2016 for details).

				Weighting				Growth	
	Half M	CPUE	CPUE2	CSLF	Model	Staircase	Negative	Weight	Others
Models									
i_0.0	No	0.10	0.08	F	Exp	Yes	Yes	No	
i_0.1	Yes	0.10	0.08	F	Exp	Yes	Yes	No	
i_0.4	Yes	0.10	0.08	F	Inv	Yes	Yes	No	
i_0.4ext	Yes	0.10	0.08	F	Inv	Yes	Yes	No	2–170mm
i_0.5	Yes	0.10	0.08	F	Inv	No	Yes	No	
i_0.5ext	Yes	0.10	0.08	F	Inv	No	Yes	No	2–170mm
i_0.6	Yes	0.10	0.08	F	Inv	No	No	No	
i_0.7	Yes	0.10	0.08	F	Inv	No	No	Yes	
i_0.7b	Yes	0.10	0.08	F	Inv	No	No	Yes	Fighting Bay LF
i_0.9	Yes	0.10	0.08	M	Inv	No	No	Yes	
i_0.11	Yes	0.10	0.08	F	Inv	No	No	Yes	Alternative catch
i_0.12	Yes	0.10	0.08	F	Inv	No	No	Yes	Alt PCELR
i_0.13	Yes	0.05	–	F	Inv	No	No	Yes	Combined CPUE

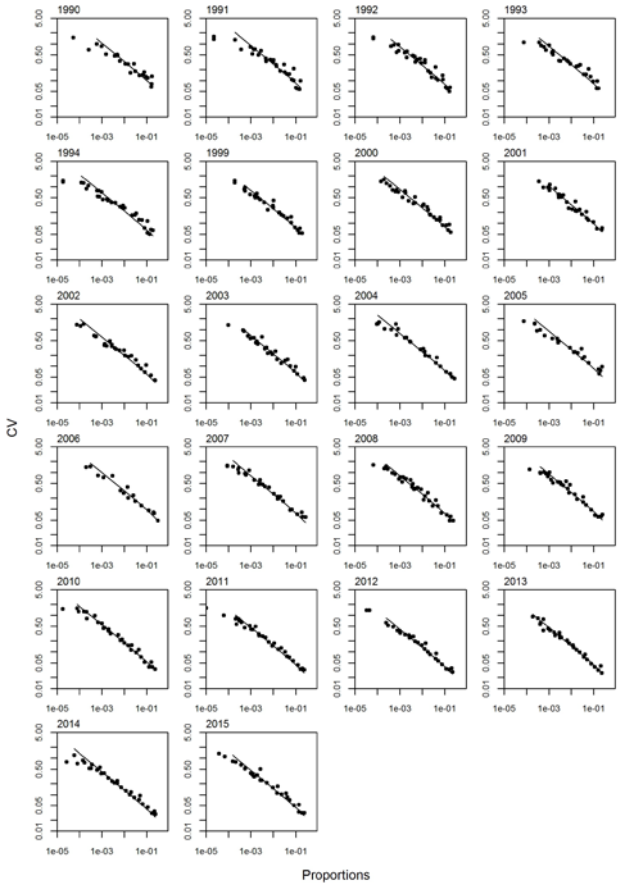

Figure A1: Estimated proportions versus CVs for the commercial catch length frequencies for PAU 7 south. Lines indicate the best least squares fit for the effective sample size of the multinomial distribution.

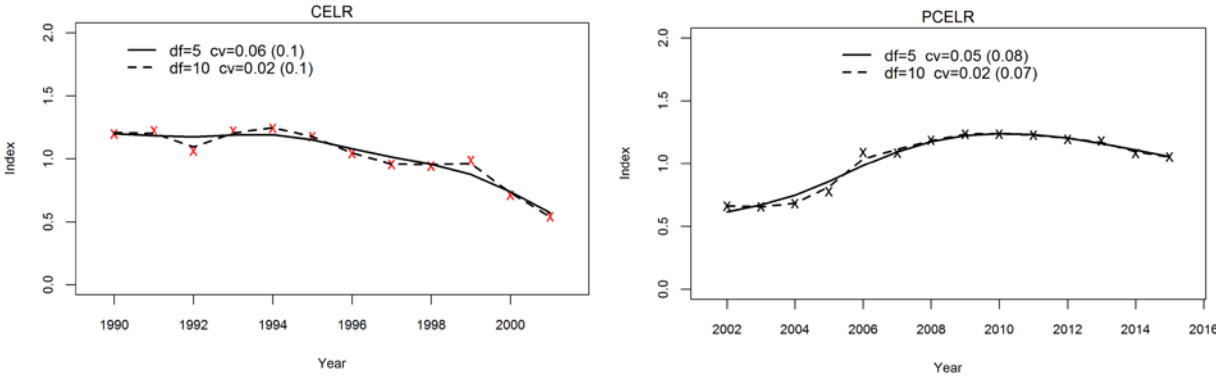

Figure A2: A series of lowess lines of various degrees of freedom (f) fitted to the PAU 7 standardised CPUE indices for 1990–2001 (left) and for 2002–2015 (right). CVs are calculated from residuals for each of the fitted lowess lines and are further adjusted for the degree of "smoothing" (adjusted value in the brackets). The CV of the "appropriate" fit will be used as the CV in the stock assessment model. What is "appropriate" is judged by visual examination of lines with different degrees of smoothing.

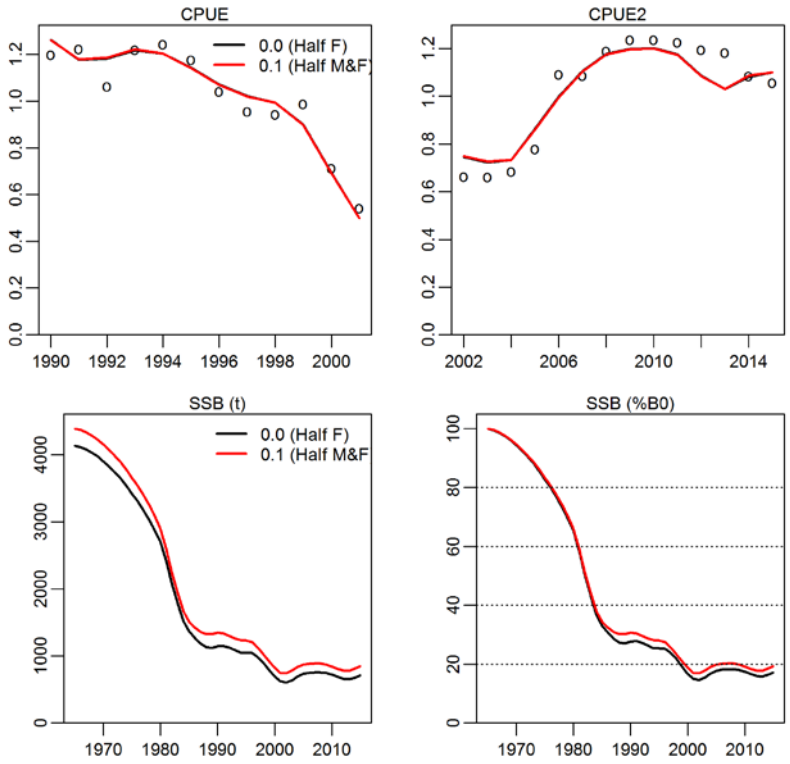

Figure A3: Comparison between initial model runs 0.0 and 0.1: Fits to the CPUE 1990–2001 (top left) and 2002–2014 (top right), estimated SSB (bottom left) and SSB as a percentage of B_0 (Bottom right).

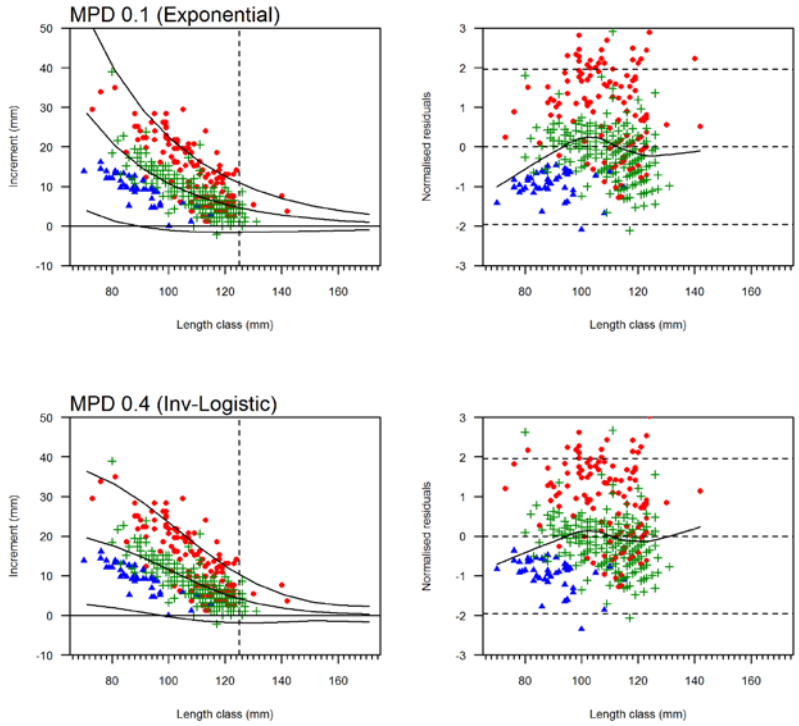

Figure A4: Comparison between initial model runs 0.1 and 0.4: Fits to tag-capture observations using exponential growth model (0.1) or inverse-logistic model (0.4) (right, lines are estimated mean growth and 90% CI), and standardised residuals from the fits (left, lines are fitted smoother). Red are observations from Rununder and Perano, Green from Northern faces, and Blue from the Staircase.

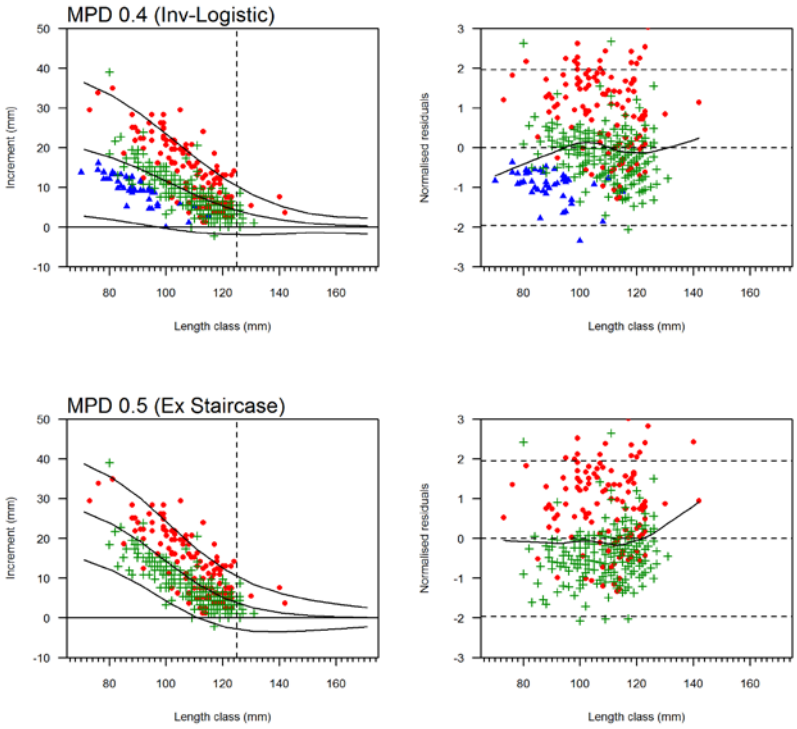

Figure A5: Comparison between initial model runs 0.4 and 0.5: fits to tag-capture observations (right, lines are estimated mean growth and 90% CI), and standardised residuals from the fits (left, lines are fitted smoother). Red are observations collected from Rununder and Perano, Green from Northern faces, and Blue from the Staircase.

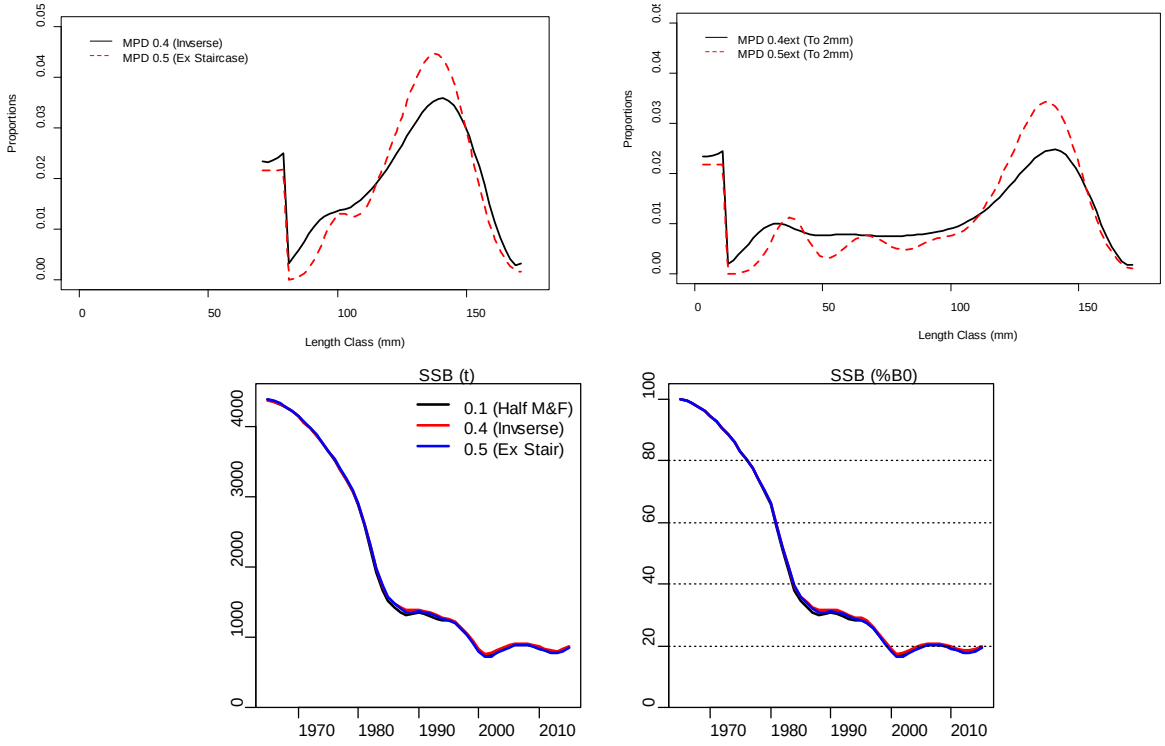

Figure A6: Comparison between initial model runs 0.4, 0.4ext, 0.5, and 0.5ext: model predicted unfished (equilibrium) population length frequency (top left and top right), and estimated SSB (bottom left) and SSB as a percentage of B_0 (bottom right).

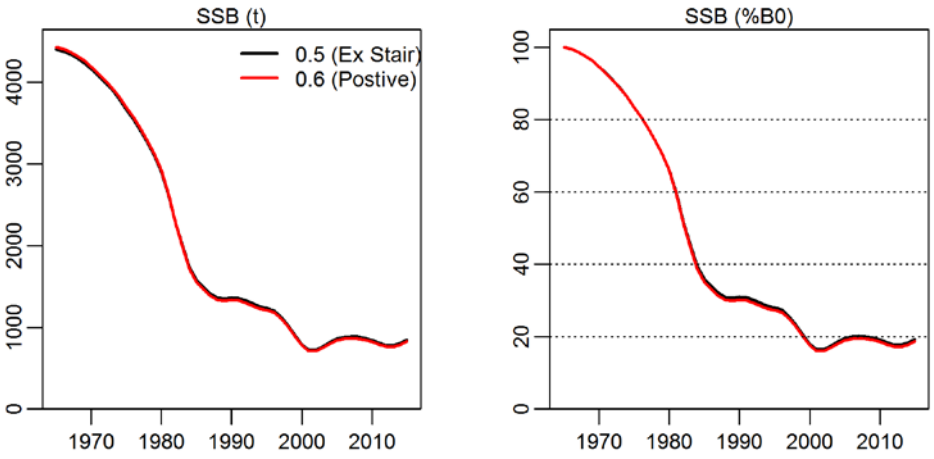

Figure A7: Comparison between initial model runs 0.5 and 0.6: estimated SSB (left) and SSB as a percentage of B_0 (Bottom right).

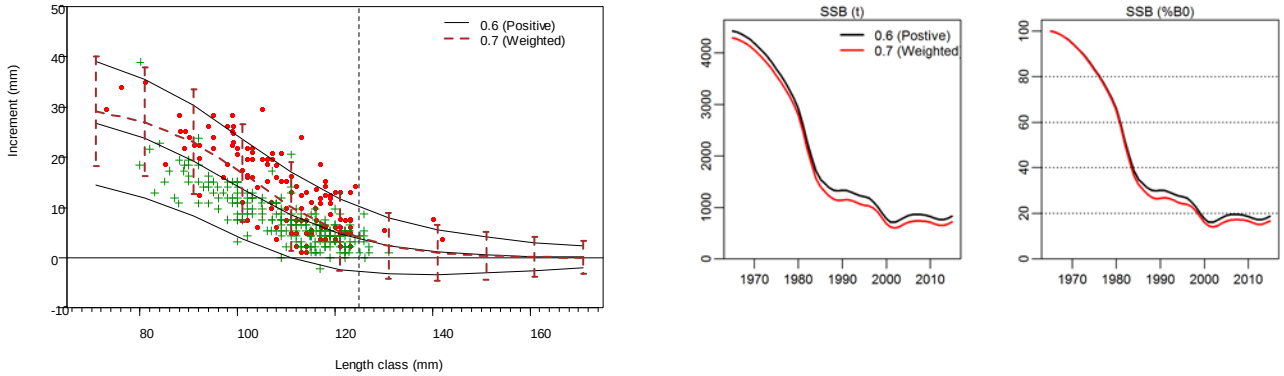

Figure A8: Comparison between initial model runs 0.6 and 0.7: fits to tag-capture observations (left, lines are estimated mean growth and 90% CI), estimated SSB (middle) and SSB as a percentage of B_0 (right). Red are observations collected from Rununder and Perano, Green from Northern faces.

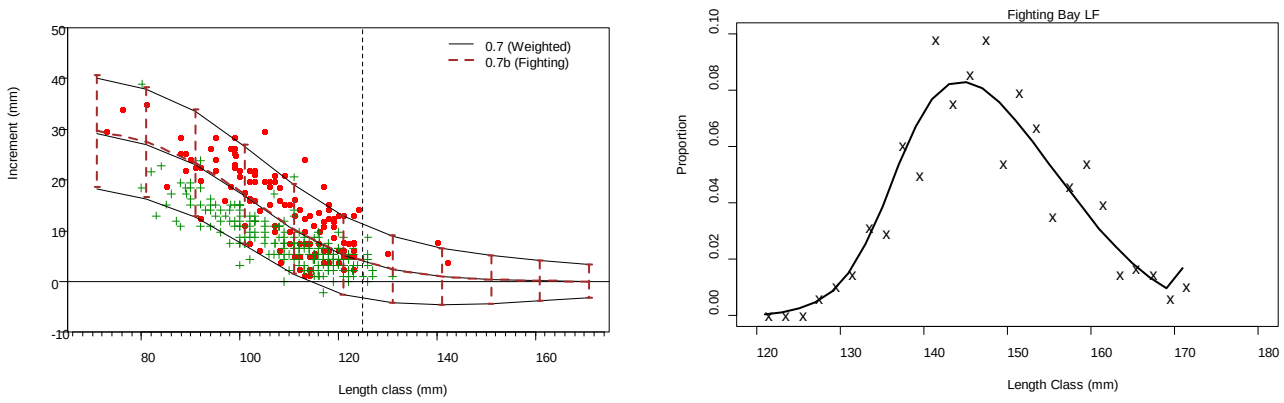

Figure A9: Comparison between initial model runs 0.7 and 0.7b: fits to tag-capture observations (left, lines are estimated mean growth and 90% CI), and fits to FBLF from run 0.7b (right).

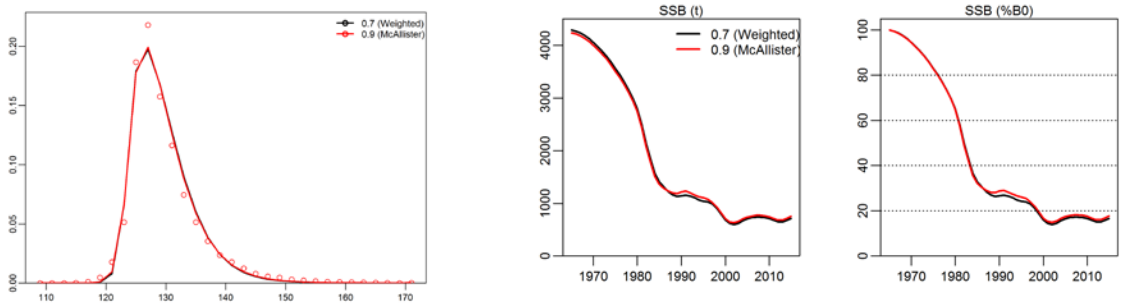

Figure A10: Comparison between initial runs 0.7 and 0.9: fits to CSLF data (left, observed and predicted values were average over all years), estimated SSB (middle) and SSB as a percentage of B_0 (right).

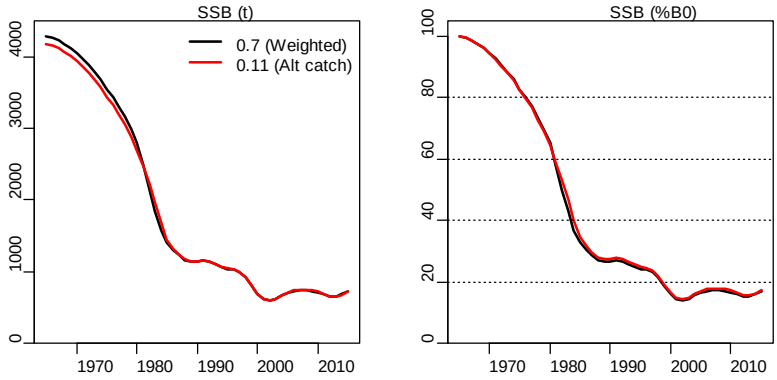

Figure A11: Comparison between runs 0.7 and 0.11: SSB (left) and SSB as a percentage of B_0 (right).

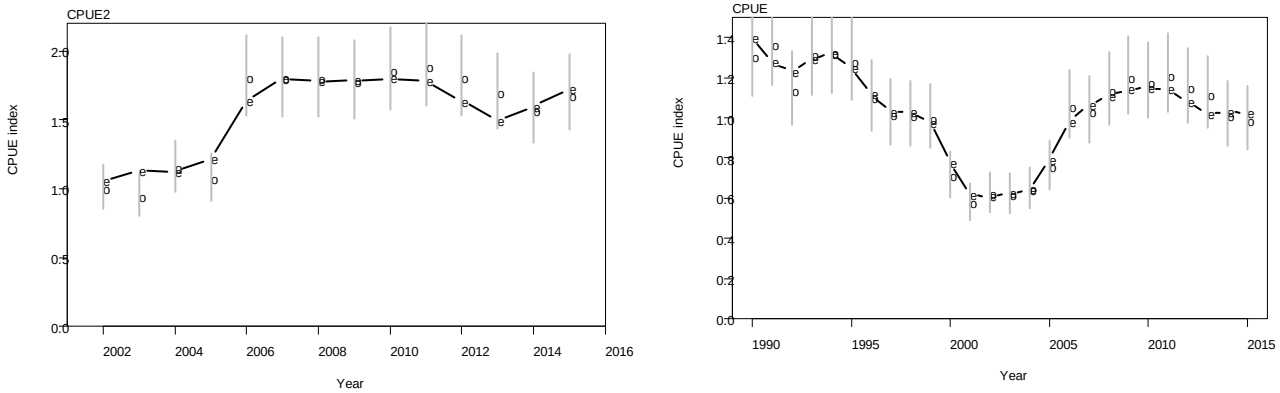

Figure A12: Fits to the alterative PCELR CPUE indices 2002–2015 by Neubauer (2015) from initial run 0.12 (left), and fits to the CELR/PCELR combined indices 1990–2015 (see Fu et al. 2016) from initial run 0.13. Vertical lines represent 95% confidence interval of observed CPUE.

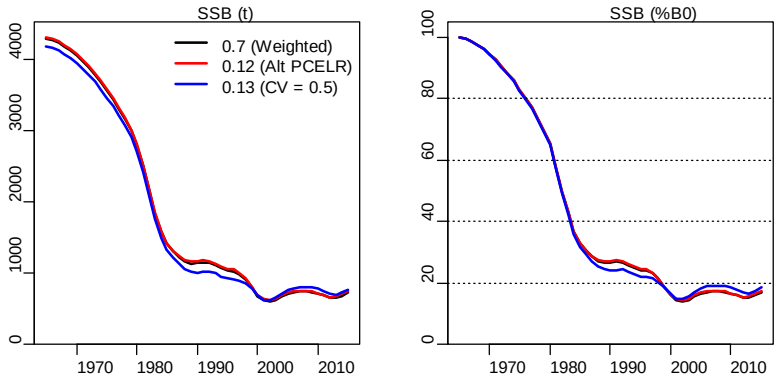

Figure A13: Comparison between runs 0.7, 0.12, and 0.13: SSB (left) and SSB as a percentage of B_0 (right).

APPENDIX B: POSTERIOR DISTRIBUTION OF M FROM PAU 5A AND PUA 5B

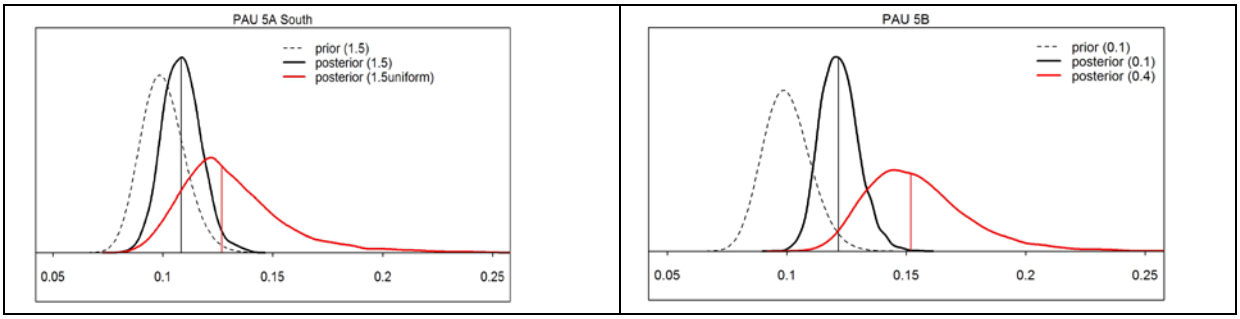

Figure B1: Posterior estimated natural mortality (M) using the base case (1.5) of the 2014 PAU 5A South assessment (Fu 2015a), and the base case (0.1) of the 2013 PAU 5B assessment (Fu 2014a), except that a uniform prior U [0.05, 0.25] was used for M. The new run is labelled as "1.5uniform" for PAU 5A, and "0.4" for PAU 5B. The dashed line is the original lognormal prior used in the base case. The vertical line is the posterior median.

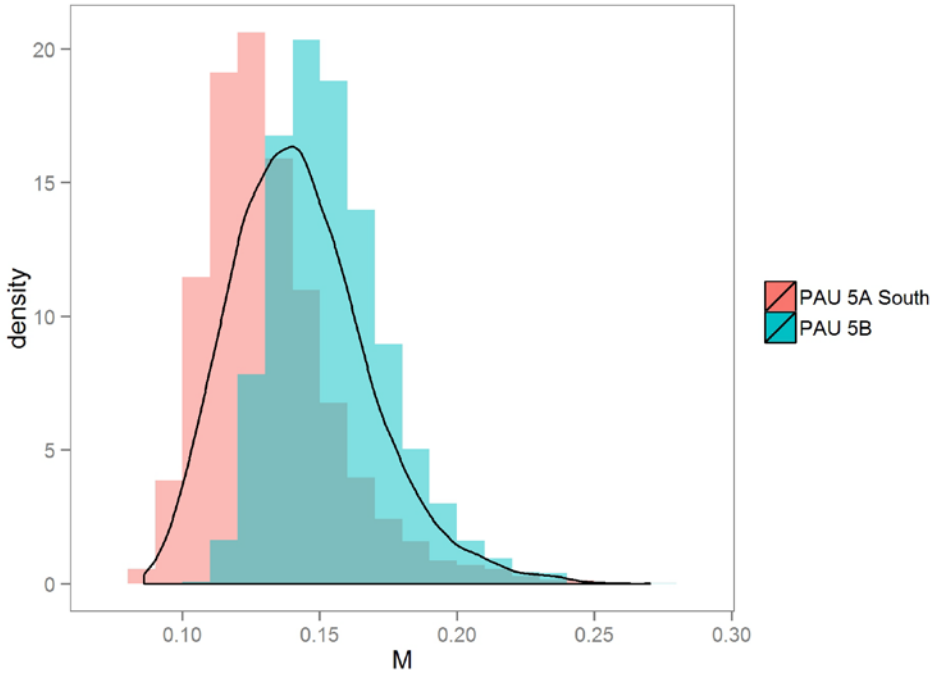

Figure B2: A lognormal distribution fitted to the combined posterior samples from the MCMC runs using a uniform prior U [0.05, 0.25] for the base case of the 2014 PAU 5A South assessment and of the 2013 PAU 5B assessment (see Figure B1). The fitted lognormal distribution has an estimated mean of 0.15 and CV of 0.17.

APPENDIX C: SUMMARY OF PROJECTIONS FOR MCMC 1.0 AND 1.4

Table C1: Summary of key indicators from the projection for the base case (MCMC 1.0) with future recruitment resampled from 2002–2011, under the catch scenario of 28% catch reduction.

	2015	2016	2017	2018
B_t	780 (676–914)	831 (681–1021)	884 (695–1120)	943 (711–1227)
$\%B_0$	0.18 (0.15–0.22)	0.19 (0.16–0.24)	0.21 (0.16–0.27)	0.22 (0.16–0.29)
$\%B_{msy}$	0.69 (0.57–0.84)	0.73 (0.59–0.93)	0.78 (0.60–1.02)	0.83 (0.61–1.11)
Pr (>Bmsy)	0.00	0.01	0.03	0.10
Pr (>Bcurrent)	0.00	0.82	0.90	0.94
Pr (>40%B0)	0.00	0.00	0.00	0.00
Pr (<20%B0)	0.83	0.61	0.41	0.26
Pr (<10%B0)	0.00	0.00	0.00	0.00
rB_t	300 (252–360)	339 (277–411)	380 (302–473)	422 (316–553)
$\%rB_0$	0.085 (0.069–0.107)	0.096 (0.075–0.123)	0.108 (0.083–0.141)	0.120 (0.086–0.163)
$\%rB_{msy}$	0.55 (0.41–0.79)	0.62 (0.45–0.90)	0.7 (0.5–1.0)	0.78 (0.53–1.16)
Pr (>rBmsy)	0.00	0.01	0.03	0.11
Pr (>rBcurrent)	0.00	1.00	1.00	1.00
Pr (U>U40%B0)	1.00	1.00	1.00	1.00

Table C2: Summary of key indicators from the projection for the base case (MCMC 1.0) with future recruitment resampled from 2002–2011, under the catch scenario of 35% catch reduction.

	2015	2016	2017	2018
B_t	780 (676–914)	836 (687–1027)	900 (712–1136)	971 (739–1255)
$\%B_0$	0.18 (0.15–0.22)	0.20 (0.16–0.25)	0.21 (0.16–0.27)	0.23 (0.17–0.30)
$\%B_{msy}$	0.69 (0.57–0.84)	0.74 (0.59–0.93)	0.80 (0.62–1.04)	0.86 (0.64–1.13)
Pr (>Bmsy)	0.00	0.01	0.04	0.14
Pr (>Bcurrent)	0.00	0.86	0.94	0.97
Pr (>40%B0)	0.00	0.00	0.00	0.00
Pr (<20%B0)	0.83	0.58	0.35	0.19
Pr (<10%B0)	0.00	0.00	0.00	0.00
rB_t	300 (252–360)	344 (282–417)	395 (317–488)	447 (341–577)
$\%rB_0$	0.085 (0.069–0.107)	0.098 (0.077–0.125)	0.112 (0.087–0.145)	0.127 (0.093–0.171)
$\%rB_{msy}$	0.55 (0.41–0.79)	0.63 (0.46–0.91)	0.73 (0.53–1.05)	0.83 (0.57–1.22)
Pr (>rBmsy)	0.00	0.01	0.04	0.16
Pr (>rBcurrent)	0.00	1.00	1.00	1.00
Pr (U>U40%B0)	1.00	1.00	1.00	0.99

Table C3: Summary of key indicators from the projection for the base case (MCMC 1.0) with future recruitment resampled from 2002–2011, under the catch scenario of 40% catch reduction.

	2015	2016	2017	2018
B_t	780 (676–914)	840 (691–1031)	912 (724–1148)	990 (759–1274)
$\%B_0$	0.18 (0.15–0.22)	0.20 (0.16–0.25)	0.21 (0.17–0.28)	0.23 (0.17–0.30)
$\%B_{msy}$	0.69 (0.57–0.84)	0.74 (0.60–0.94)	0.81 (0.63–1.05)	0.88 (0.65–1.15)
Pr (>Bmsy)	0.00	0.01	0.05	0.17
Pr (>Bcurrent)	0.00	0.88	0.96	0.98
Pr (>40%B0)	0.00	0.00	0.00	0.00
Pr (<20%B0)	0.83	0.57	0.32	0.15
Pr (<10%B0)	0.00	0.00	0.00	0.00
rB_t	300 (252–360)	348 (286–420)	406 (328–499)	464 (359–595)
$\%rB_0$	0.085 (0.069–0.107)	0.099 (0.078–0.126)	0.12 (0.09–0.15)	0.132 (0.098–0.176)
$\%rB_{msy}$	0.55 (0.41–0.79)	0.64 (0.47–0.92)	0.75 (0.54–1.08)	0.86 (0.60–1.25)
Pr (>rBmsy)	0.00	0.01	0.05	0.21
Pr (>rBcurrent)	0.00	1.00	1.00	1.00
Pr (U>U40%B0)	1.00	1.00	1.00	0.98

Table C4: Summary of key indicators from the projection for the base case (MCMC 1.0) with future recruitment resampled from 2002–2011, under the catch scenario of 50% catch reduction.

	2015	2016	2017	2018
B_t	780 (676–914)	848 (699–1039)	936 (749–1172)	1030 (799–1314
$\%B_0$	0.18 (0.15–0.22)	0.20 (0.16–0.25)	0.22 (0.17–0.28)	0.24 (0.18–0.31)
$\%B_{msy}$	0.69 (0.57–0.84)	0.75 (0.60–0.94)	0.83 (0.65–1.07)	0.91 (0.69–1.18)
Pr (>Bmsy)	0.00	0.01	0.07	0.24
Pr (>Bcurrent)	0.00	0.91	0.98	0.99
Pr (>40%B0)	0.00	0.00	0.00	0.00
Pr (<20%B0)	0.83	0.53	0.24	0.09
Pr (<10%B0)	0.00	0.00	0.00	0.00
rB_t	300 (252–360)	355 (293–428)	428 (350–521)	500 (395–631)
$\%rB_0$	0.085 (0.069–0.107)	0.10 (0.08–0.13)	0.121 (0.096–0.155)	0.14 (0.11–0.19)
$\%rB_{msy}$	0.55 (0.41–0.79)	0.66 (0.48–0.94)	0.79 (0.58–1.12)	0.93 (0.66–1.33)
Pr (>rBmsy)	0.00	0.01	0.09	0.33
Pr (>rBcurrent)	0.00	1.00	1.00	1.00
Pr (U>U40%B0)	1.00	1.00	0.98	0.83

Table C5: Summary of key indicators from the projection for the base case (MCMC 1.0) with future recruitment resampled from 2002–2011, under the catch scenario of current TACC.

B_t	780 (676–914)	808 (659–999)	817 (628–1054)	832 (599–1118)
$\%B_0$	0.18 (0.15–0.22)	0.19 (0.15–0.24)	0.19 (0.14–0.25)	0.19 (0.14–0.27)
$\%B_{msy}$	0.69 (0.57–0.84)	0.72 (0.57–0.91)	0.72 (0.54–0.96)	0.74 (0.52–1.01)
Pr (>Bmsy)	0.00	0.00	0.01	0.03
Pr (>Bcurrent)	0.00	0.67	0.66	0.68
Pr (>40%B0)	0.00	0.00	0.00	0.00
Pr (<20%B0)	0.83	0.69	0.62	0.57
Pr (<10%B0)	0.00	0.00	0.00	0.00
rB_t	300 (252–360)	318 (256–392)	319 (240–412)	322 (216–455)
$\%rB_0$	0.085 (0.069–0.107)	0.09 (0.07–0.12)	0.091 (0.066–0.123)	0.092 (0.059–0.133)
$\%rB_{msy}$	0.55 (0.41–0.79)	0.59 (0.42–0.85)	0.59 (0.40–0.88)	0.60 (0.36–0.95)
Pr (>rBmsy)	0.00	0.00	0.01	0.01
Pr (>rBcurrent)	0.00	0.98	0.78	0.66
Pr (U>U40%B0)	1.00	1.00	1.00	1.00

Table C6: Summary of key indicators from the projection for the base case (MCMC 1.0) with future recruitment resampled from 2010–2011, under the catch scenario of 28% catch reduction.

	2015	2016	2017	2018
B_t	780 (676–914)	790 (662–940)	807 (642–994)	822 (621–1050)
$\%B_0$	0.18 (0.15–0.22)	0.18 (0.15–0.23)	0.19 (0.15–0.24)	0.19 (0.14–0.25)
$\%B_{msy}$	0.69 (0.57–0.84)	0.70 (0.57–0.86)	0.71 (0.55–0.90)	0.73 (0.54–0.96)
Pr (>Bmsy)	0.00	0.00	0.00	0.01
Pr (>Bcurrent)	0.00	0.60	0.66	0.67
Pr (>40%B0)	0.00	0.00	0.00	0.00
Pr (<20%B0)	0.83	0.78	0.70	0.62
Pr (<10%B0)	0.00	0.00	0.00	0.00
rB_t	300 (252–360)	337 (276–411)	367 (295–450)	388 (294–492)
$\%rB_0$	0.085 (0.069–0.107)	0.096 (0.075–0.123)	0.10 (0.08–0.13)	0.11 (0.08–0.15)
$\%rB_{msy}$	0.55 (0.41–0.79)	0.62 (0.45–0.89)	0.68 (0.48–0.98)	0.72 (0.49–1.05)
Pr (>rBmsy)	0.00	0.01	0.02	0.04
Pr (>rBcurrent)	0.00	1.00	1.00	1.00
Pr (U>U40%B0)	1.00	1.00	1.00	1.00

Table C7: Summary of key indicators from the projection for the base case (MCMC 1.0) with future recruitment resampled from 2010–2011, under the catch scenario of 40% catch reduction.

	2015	2016	2017	2018
B_t	780 (676–914)	799 (672–950)	835 (671–1022)	869 (669–1096)
$\%B_0$	0.18 (0.15–0.22)	0.19 (0.15–0.23)	0.20 (0.15–0.25)	0.20 (0.15–0.26)
$\%B_{msy}$	0.69 (0.57–0.84)	0.71 (0.57–0.87)	0.74 (0.58–0.93)	0.77 (0.58–1.00)
Pr (>Bmsy)	0.00	0.00	0.01	0.02
Pr (>Bcurrent)	0.00	0.70	0.81	0.84
Pr (>40%B0)	0.00	0.00	0.00	0.00
Pr (<20%B0)	0.83	0.75	0.59	0.45
Pr (<10%B0)	0.00	0.00	0.00	0.00
rB_t	300 (252–360)	346 (285–419)	393 (322–476)	431 (338–534)
$\%rB_0$	0.085 (0.069–0.107)	0.098 (0.077–0.125)	0.112 (0.088–0.142)	0.122 (0.09–0.158)
$\%rB_{msy}$	0.55 (0.41–0.79)	0.64 (0.47–0.91)	0.73 (0.53–1.04)	0.80 (0.56–1.14)
Pr (>rBmsy)	0.00	0.01	0.04	0.10
Pr (>rBcurrent)	0.00	1.00	1.00	1.00
Pr (U>U40%B0)	1.00	1.00	1.00	0.99

Table C8: Summary of key indicators from the projection for the base case (MCMC 1.0) with future recruitment resampled from 2010–2011, under the catch scenario of 50% catch reduction.

	2015	2016	2017	2018
B_t	780 (676–914)	807 (680–958)	859 (695–1045)	908 (709–1135)
$\%B_0$	0.18 (0.15–0.22)	0.19 (0.15–0.23)	0.20 (0.16–0.25)	0.21 (0.16–0.27)
$\%B_{msy}$	0.69 (0.57–0.84)	0.71 (0.58–0.88)	0.76 (0.60–0.95)	0.80 (0.61–1.03)
Pr (>Bmsy)	0.00	0.00	0.01	0.02
Pr (>Bcurrent)	0.00	0.70	0.81	0.84
Pr (>40%B0)	0.00	0.00	0.00	0.00
Pr (<20%B0)	0.83	0.75	0.59	0.45
Pr (<10%B0)	0.00	0.00	0.00	0.00
rB_t	300 (252–360)	353 (292–426)	415 (344–498)	467 (374–570)
$\%rB_0$	0.085 (0.069–0.107)	0.100 (0.079–0.128)	0.118 (0.093–0.149)	0.13 (0.10–0.17)
$\%rB_{msy}$	0.55 (0.41–0.79)	0.65 (0.48–0.93)	0.77 (0.56–1.08)	0.86 (0.62–1.22)
Pr (>rBmsy)	0.00	0.01	0.04	0.10
Pr (>rBcurrent)	0.00	1.00	1.00	1.00
Pr (U>U40%B0)	1.00	1.00	1.00	0.99

Table C9: Summary of key indicators from the projection for MCMC 1.4 with future recruitment resampled from 2010–2011, under the catch scenario of 28% catch reduction.

	2015	2016	2017	2018
B_t	821 (708–963)	826 (695–979)	840 (681–1024)	850 (658–1069)
$\%B_0$	0.22 (0.17–0.29)	0.22 (0.17–0.30)	0.22 (0.17–0.30)	0.23 (0.16–0.31)
$\%B_{msy}$	0.81 (0.63–1.00)	0.81 (0.63–1.02)	0.83 (0.62–1.06)	0.84 (0.61–1.10)
Pr (>Bmsy)	0.03	0.04	0.07	0.11
Pr (>Bcurrent)	0.00	0.55	0.63	0.63
Pr (>40%B0)	0.00	0.00	0.00	0.00
Pr (<20%B0)	0.30	0.28	0.25	0.23
Pr (<10%B0)	0.00	0.00	0.00	0.00
rB_t	306 (259–361)	350 (289–420)	386 (314–464)	406 (318–503)
$\%rB_0$	0.102 (0.077–0.140)	0.116 (0.085–0.164)	0.128 (0.093–0.182)	0.135 (0.09–0.193)
$\%rB_{msy}$	0.74 (0.48–1.20)	0.85 (0.54–1.39)	0.94 (0.58–1.54)	0.99 (0.60–1.63)
Pr (>rBmsy)	0.17	0.30	0.41	0.49
Pr (>rBcurrent)	0.00	1.00	1.00	1.00
Pr (U>U40%B0)	0.99	0.94	0.87	0.84

Table C10: Summary of key indicators from the projection for MCMC 1.4 with future recruitment resampled from 2010–2011, under the catch scenario of 40% catch reduction.

B_t	821 (708–963)	836 (705–989)	868 (709–1052)	897 (705–1114)
$\%B_0$	0.22 (0.17–0.29)	0.22 (0.17–0.30)	0.23 (0.17–0.31)	0.24 (0.17–0.32)
$\%B_{msy}$	0.81 (0.63–1.00)	0.82 (0.64–1.03)	0.86 (0.65–1.09)	0.88 (0.65–1.15)
Pr (>Bmsy)	0.03	0.05	0.11	0.18
Pr (>Bcurrent)	0.00	0.66	0.79	0.81
Pr (>40%B0)	0.00	0.00	0.00	0.00
Pr (<20%B0)	0.30	0.25	0.18	0.14
Pr (<10%B0)	0.00	0.00	0.00	0.00
rB_t	306 (259–361)	359 (298–428)	412 (340–490)	448 (361–545)
$\%rB_0$	0.102 (0.077–0.140)	0.119 (0.088–0.168)	0.14 (0.10–0.19)	0.15 (0.11–0.21)
$\%rB_{msy}$	0.74 (0.48–1.20)	0.87 (0.55–1.43)	1.00 (0.63–1.63)	1.09 (0.68–1.78)
Pr (>rBmsy)	0.17	0.33	0.50	0.62
Pr (>rBcurrent)	0.00	1.00	1.00	1.00
Pr (U>U40%B0)	0.99	0.86	0.73	0.63

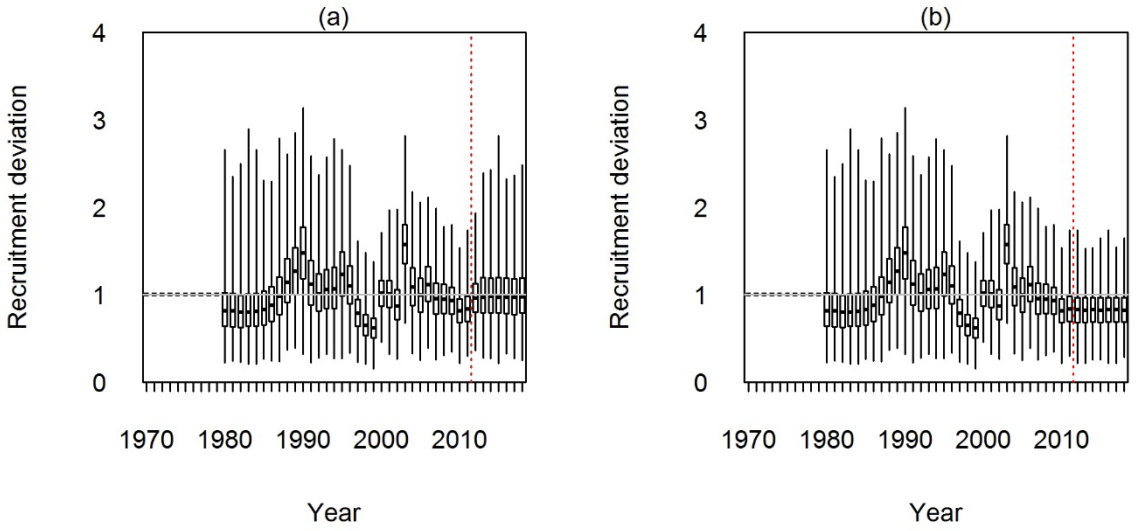

Figure C1: Randomised recruitment used for the projections, where recruitment for 2012–2018 were resampled from (a) 2002–2011 (average recruitment), or (b) 2010–2011 (low recruitment). The vertical dashed line indicates when the randomisations started.

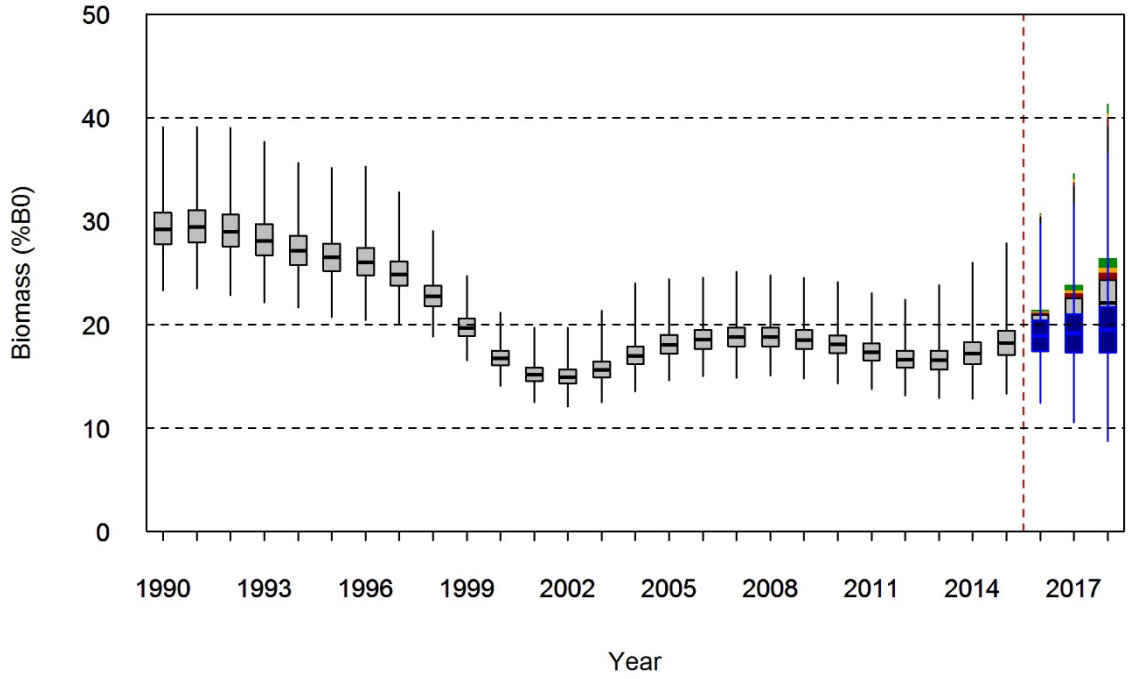

Figure C2: Posterior distributions of projected spawning stock biomass 2016–2018 for the base case (MCMC 1.0) with future recruitment resampled from model estimates 2002–2011 under five catch scenarios: 28% catch reduction (black), 35% reduction (red), 40% reduction (orange), and current TACC (blue), and 50% reduction (green). The box shows the median of the posterior distribution (horizontal bar), the 25th and 75th percentiles (box), with the whiskers representing the full range of the distribution.

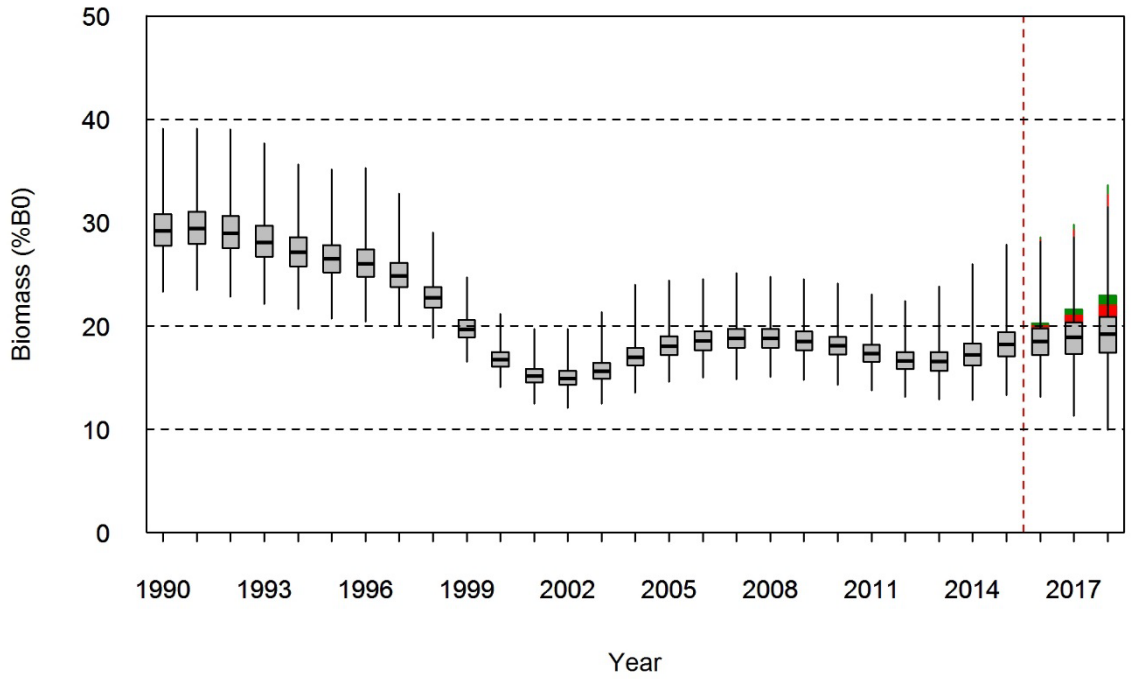

Figure C3: Posterior distributions of projected spawning stock biomass 2016–2018 for the base case (MCMC 1.0) with future recruitment resampled from model estimates 2010–2011 under three catch scenarios: 28% catch reduction (black), 40% reduction (red), and 50% reduction (green). The box shows the median of the posterior distribution (horizontal bar), the 25th and 75th percentiles (box), with the whiskers representing the full range of the distribution.

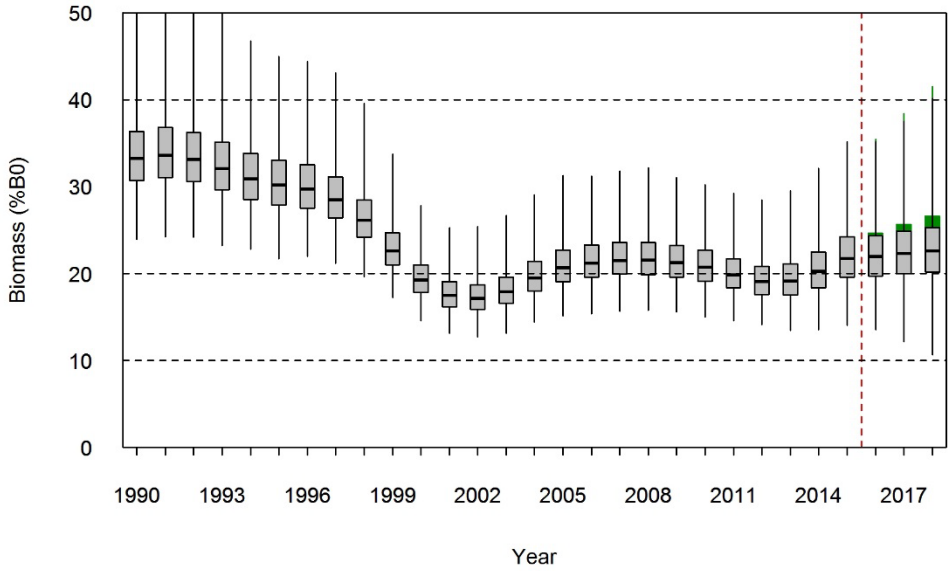

Figure C4: Posterior distributions of projected spawning stock biomass 2016–2018 for MCMC 1.4 with future recruitment resampled from model estimates 2010–2011 under two catch scenarios: 28% catch reduction (black) and 40% reduction (green). The box shows the median of the posterior distribution (horizontal bar), the 25th and 75th percentiles (box), with the whiskers representing the full range of the distribution.